PHASE VARIABILITY OF
STRUCTURAL TRANSFER FUNCTIONS

by

Robert Gould Gibson

B.S.E., Princeton University

(1984)

SUBMITTED IN PARTIAL FULFILLMENT OF THE

REQUIREMENTS OF THE DEGREE OF

MASTER OF SCIENCE

IN MECHANICAL ENGINEERING

at the

MASSACHUSETTS INSTITUTE OF TECHNOLOGY

February 1986

© Massachusetts Institute of Technology 1986

Signature of Author _____
Department of Mechanical Engineering
February 27, 1986

Certified by _____
Richard H. Lyon
Thesis Supervisor

Accepted by _____
Ain Sonin
Chairman, Graduate Commitee

MASSACHUSETTS INSTITUTE OF TECHNOLOGY

JUL 28 1986

LIBRARIES Archives

PHASE VARIABILITY OF STRUCTURAL TRANSFER FUNCTIONS

by

ROBERT GOULD GIBSON

Submitted to the Department of Mechanical Engineering on February 27, 1986 in partial fulfillment of the requirements for the Degree of Master of Science in Mechanical Engineering

ABSTRACT

Transfer functions have been measured on a large number of machine structures in order to study the feasibility of a robust inverse filter for use in fault diagnosis in machinery. The structures consisted of fully assembled diesel engines, engines on an assembly line, and engine castings. Transfer functions were determined by applying a force from a mechanical shaker to one point on a structure and measuring the acceleration at another point. Simple ensemble statistics were applied to the data to assess the amount of variability in the magnitude and phase of the transfer functions of identical machines.

Using previously developed theories for the frequency dependence of transfer function phase, a random walk model was developed to explain phase behavior and to predict the level of phase variability. Although the data seem relatively consistent with the existing theory, especially when compared to previously measured transfer functions, the model cannot predict values of unwrapped phase or levels of variability with much precision. It appears that the level of phase variability is too high for a single inverse filter to be successfully applied to a group of identical machines.

In an attempt to account for the deviation between theory and data, the phase features of individual transfer functions were examined. Some evidence was found to suggest the possibility of non-minimum-phase behavior of structural transfer functions.

Thesis Supervisor: Richard H. Lyon

Title: Professor of Mechanical Engineering

ACKNOWLEDGEMENTS

Thanks to Professor Lyon for his patient guidance throughout this work.

Thanks to David Bowen and Jeung Kim, who accompanied me to Columbus, Indiana to aid in the collection of experimental data. Also thanks to Jeung for his discussions and helpful suggestions.

Thanks to Greg Chisholm, Steve Petri, and the other members of the A&V Lab who helped in my understanding of instrumentation and computing.

Thanks to Marie-Louise Murville who provided advice during the initial stages of my work.

Thanks to Dave Reid and Fred Nerz of Cummins Engine Company for their continued interest in and support of this research.

Thanks to Mary Toscano for looking after all the details.

This work was sponsored by National Science Foundation grant # 8400636-MEA and by Cummins Engine Company, Inc.

TABLE OF CONTENTS

LIST OF FIGURES

CHAPTER 1

AN INTRODUCTION TO MACHINERY DIAGNOSTICS

A common technique for identifying flaws in structures or machinery is the analysis of vibration. Any operating machine or structure excited by an applied force will have certain natural vibration characteristics which can be measured either on the surface or in the radiated sound field. A mechanic, experienced in observing the operation of a particular machine, can often diagnose an operating fault after noticing a change in the machine's sound or vibration. The situation is similar in the case of non-operating structures; an experienced founder can detect mistunings or locate cracks in a bell by applying a force, such as a blow from the bell's clapper, and observing the resulting sound. This method of evaluation is particularly valuable because through its use faults can be detected inexpensively and without disassembling the machine.

1.1 INVERSE FILTERING

In an effort to automate these diagnostic techniques, vibration can be measured at a single point on the structure and compared to a force input. When the data are examined in the spectral form, or frequency domain, the ratio of output to input is known as a transfer function, or alternatively, a frequency response;

$$H(\omega) = O(\omega) \; / \; I(\omega) \qquad (1.1)$$

where $I(\omega)$ is the input spectrum, $O(\omega)$ is the output spectrum, and $H(\omega)$ is the transfer function. In machinery, the input force usually originates at an interior point, inaccessible to an observer or to measuring instruments. Thus the transfer function, once it has been determined, provides a simple relationship between easily measurable vibration data and internal operating characteristics.

The primary value of the transfer function is in its use as an inverse filter. When Equation 1.1 is rewritten as

$$O(\omega) = I(\omega) \times H(\omega) \qquad (1.2)$$

it states that the output vibration spectrum is equal to the input force spectrum multiplied by the transfer function, which acts as a filter. The transfer function can be determined by simultaneously measuring force and vibration on a specially instrumented machine. Once these filter characteristics are known, the input force need not be measured again since its spectrum can be determined from the product of the vibration spectrum and the inverse transfer function;

$$I(\omega) = O(\omega) \times H^{-1}(\omega) \qquad (1.3)$$

With successful inverse filtering, internal forces can be monitored simply by monitoring external vibrations, a much less expensive measurement.

Inverse filtering has been used very successfully to reconstruct input time signatures from vibration data. In experiments by Ordubadi, the combustion pressure signal within an engine cylinder has been recovered solely from engine casing vibration [1]. Vibration has also been used to differentiate a faulty valve impact from a proper one [2]. Ordubadi showed that, of the two parts of a transfer function, the phase is much more important than the magnitude for use as a signature inverse filter. Therefore this study concentrates on the phase of transfer functions.

A disadvantage of inverse filtering is that the transfer function must be known quite accurately in order to correctly reproduce the input. Ordubadi's work shows that sufficient accuracy can be easily obtained when only one machine is considered. However, it is desirable to be able to apply that same transfer function to all machines made to the same specifications since the determination of the transfer function is an expensive process. The goal of much current research is to determine how to generalize the inverse filtering process from one machine to an ensemble of identical machines. A filter that is applicable to a large number of machines is called a robust filter.

Recent research by Murville [3] examined a large group of new machines, identically manufactured diesel engines. These engines were not run at the time of test, but were treated as non-operating structures. To each engine, an external force was applied and a transfer function measured. A sample transfer function is shown in Figure 1.1. It was found that both the magnitude and the phase of the transfer functions varied considerably from structure to structure, even under controlled experimental conditions. Murville's work suggests that a single inverse filter cannot be applied to an ensemble of machines.

The goal of this thesis is to examine further the variability phenomena observed by Murville, especially the variations in the transfer function phase. Additional experiments have been conducted and some statistics applied to quantify the variability of structures. Although no signature inverse filtering was attempted, the examination of transfer functions has implications for diagnostics as well. A flawed structure, such as a cracked engine block, would hopefully have a transfer function which would deviate considerably from those of a group of sound structures. The variability of the transfer functions of structures which are known to be sound can provide a standard against which the transfer function of a sample structure can be measured. The knowledge obtained from the study of variability of identical machine structures may help in the identification of faulty machines, since a simple transfer function measurement could then be used as a

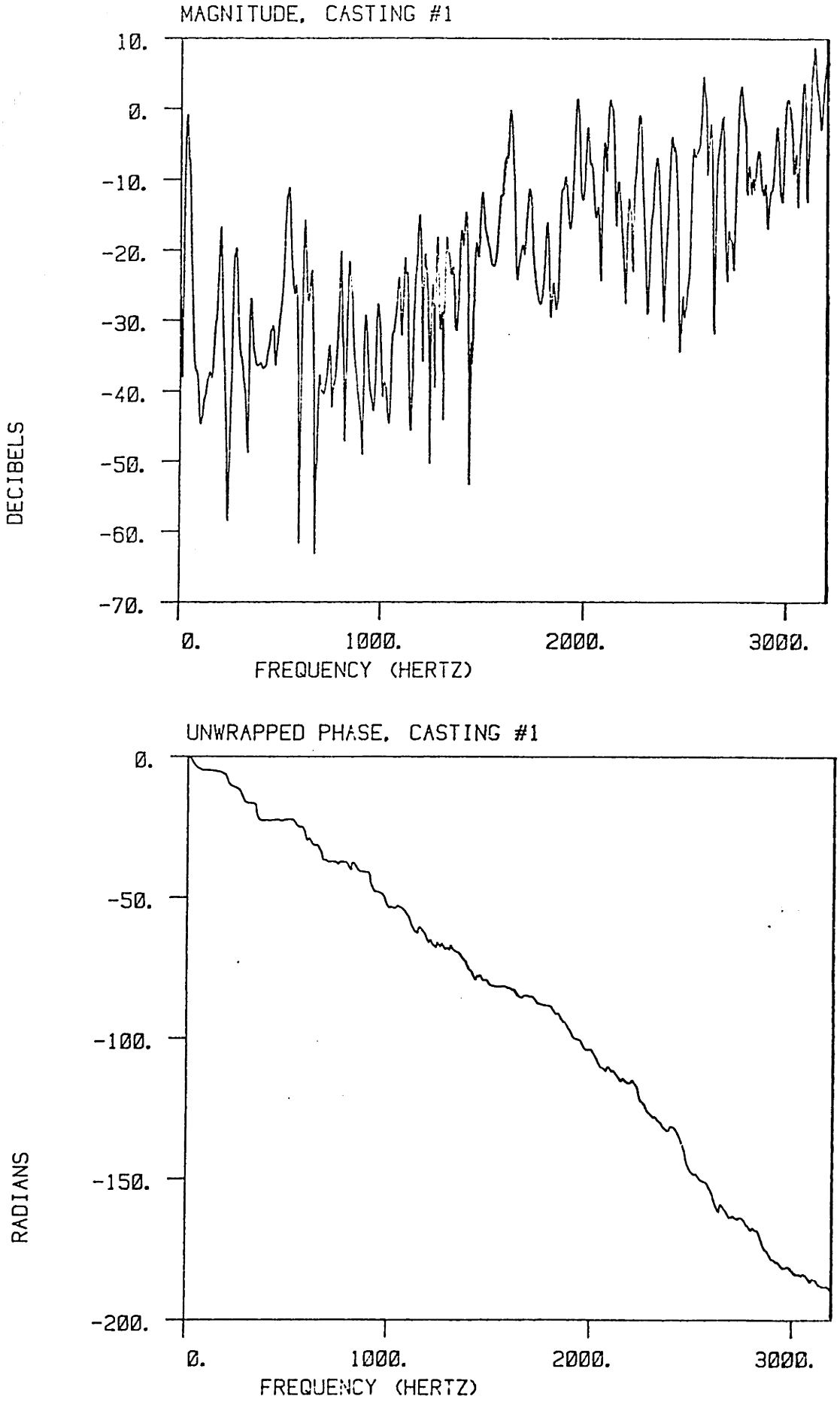

FIGURE 1.1 - Sample Casting Transfer Function (1985)

method for fault identification.

1.2 FREQUENCY DOMAIN ANALYSIS

Progress has been rapid in acoustics and vibrations research over the last decade largely on account of the arrival on the market of low-cost circuitry for performing rapid Fourier Analysis. Some important aspects of Fourier Analysis are reviewed here.

Vibration data are commonly examined in two forms: the time domain, in which the signal is often called a time history or a signature, and the frequency domain, where spectral content is presented. A time signal is converted into a frequency spectrum through the Fourier Transform

$$X(\omega) = \mathcal{F}\{x(t)\} \qquad (1.4)$$

where

$$\mathcal{F}\{x(t)\} = \int_{-\infty}^{\infty} x(t)\ e^{-j\omega t}\ dt \qquad (1.5)$$

A computerized analyzer employs the Discrete Fourier Transform, in which the frequency spectrum is divided into a certain number, n, of discrete frequency bands, commonly called points or lines. The n-point Fourier transform is computed from a sampled version of the time signal.

The spectrum which results from a Fourier Transform is a complex quantity; that is, it must be represented by real and imaginary components, or equivalently by magnitude and phase. Magnitude data is commonly used in engineering and is generally well understood. It represents the amplitude or

signal strength at each frequency and is easily used for detecting resonances, harmonic content, and the like. Phase spectra, however, are generally poorly understood and therefore rarely employed in engineering work. However, since phase has been shown to be essential to inverse filtering for diagnostics, it needs to be studied more closely.

1.3 THE PHASE OF TRANSFER FUNCTIONS

The phase of a transfer function represents the delay between input and output responses, expressed in angular frequency. Spectrum analyzers generally display only the principle value of the phase, a value between -pi and +pi radians. Unfortunately, this version of the phase is not particularly useful in signal processing applications due to an ambiguity inherent in knowledge of only the principle value. Phase delay often progresses beyond +/-pi in a physical system, but this information is ignored in analyzer circuitry. As an example, phase values are shown for a wave travelling down a string, in Figure 1.2.

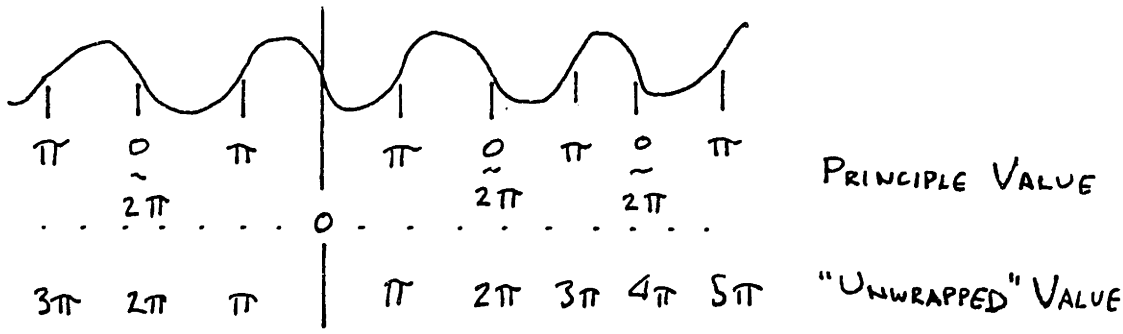

FIGURE 1.2 - Phase of wave in String

The actual phase value provides some information about the

system that the principle value does not. The process of restoring the integer multiples of 2 x pi that the analyzer has discarded is known as phase unwrapping. The process transforms the often jagged, discontinuous phase plot into a continuous function, a smooth unwrapped phase curve.

Phase unwrapping is a standard procedure which is most commonly required when cepstral analysis, a non-linear signal processing technique, is used [4]. In fact, cepstral analysis has played an important role in the development of successful machinery diagnostics [5].

The algorithm employed to unwrap phase is called adaptive numerical integration [6]. In adaptive integration, real and imaginary transfer function data are used to compute both the principle value of the phase and the phase derivative at each frequency point. Then a set of permissible phase values is defined for each frequency by adding multiples of 2 x pi to the principle value. An estimate for the phase at each frequency is then found by numerically integrating the phase derivative using an arbitrary frequency step size. The step interval is then adapted (narrowed) until the estimate agrees, to within a predefined threshold of accuracy, with one of the permissible phase values. The unwrapping is considered successful when this operation can be performed at every frequency point.

The success of phase unwrapping depends in a large part on the frequency resolution of the original data. The frequency line spacing of the data must be smaller than the frequency range over which phase fluctuates by pi radians. If this condition is not met, then either the unwrapping algorithm will fail to yield a result or the unwrapped phase curve will not accurately represent all the phase fluctuations of the true system response. This issue of frequency resolution is an important one in experimental considerations, and is addressed later in this thesis.

CHAPTER 2

THE VIBRATION OF STRUCTURES

Since the vibration of a machine in response to some force input results from the propagation of waves through the structure, it is necessary to give some attention to structural wave dynamics. †

2.1 ELEMENTARY WAVE PROPERTIES

A structure such as a diesel engine is most easily modeled, for vibration analysis, as a two-dimensional structure. That is, an engine could be idealized as a metal plate formed in the proper shape, rather than as a solid three-dimensional block. Although most sources of impact excitation occur on the machine's interior, the impact energy is readily transmitted to the structural shell, which vibrates and radiates sound as waves propagate across the machine's surface.

---

† The material in this chapter is a review of previous work by Lyon. More thorough explanation can be found in references 7, 8, and 9. The discussion is included here because the material in these papers forms the theoretical basis for much of the work in this thesis.

Of the wave types possible in a structure, the type most important in noise and vibration analysis is the bending wave, in which structural motion is perpendicular to the direction of wave propagation. An elastic structure, when excited in bending, will behave like the string previously shown in Figure 1.2; that is, a wave of any frequency will travel along the beam, and phase delay will increase with distance from the point of excitation. If the structure is finite in extent, then infinite wave propagation is not possible, and the vibration will only occur at certain resonant frequencies, determined by the structure's geometry and material properties. For a string, a dynamic system governed by the classical wave equation, the string's length must be an integer number of half-wavelengths, or

$$n \times (\lambda / 2) = L \qquad (2.1)$$

If we introduce the wave number k, where

$$k = 2 \times pi / \lambda \qquad (2.2)$$

then

$$k = n \times pi / L \qquad (2.3)$$

is the condition for resonance. Since $k = \omega/c$, where c is the speed of free wave propagation, then resonance will occur whenever

$$\omega = n \times pi \times c / L \qquad (2.4)$$

In this case, resonant modes occur at regular frequency intervals. Modes can be presented schematically on a frequency axis, as in Figure 2.1, where the x's represent resonances.

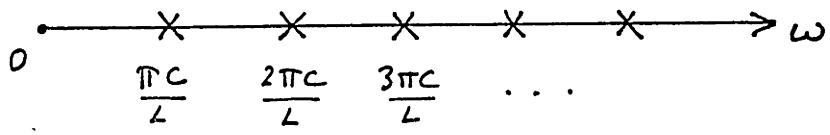

FIGURE 2.1 - Resonant Modes of a String (Equal Modal Spacing)

This condition is described as constant modal spacing.

Bending waves in a beam are not governed by the classical wave equation, but rather exhibit dispersive behavior, in which wave speed is dependent on frequency. The fundamental physical condition for resonance, expressed in Equation 2.3, must still be met, but dispersion introduces a non-linear relationship between frequency and wavenumber,

$$k^2 = \omega / (\chi \times c) \qquad (2.5)$$

where χ is the radius of gyration of the structural cross-section, proportional to the beam thickness. Since wavenumber increases as the square root of frequency, there are fewer allowable resonant wavelengths at any given frequency. Therefore modal spacing increases as the square root of frequency in one-dimensional bending.

2.2 TWO DIMENSIONAL STRUCTURES

The simplest example of a two-dimensional structure is a simply supported plate. The same dispersion relation exists, but the boundary conditions now require that both plate dimensions meet the wavelength criterion (Equation 2.1). This means that, for a square plate of side L bounded on two sides by axes x1 and x2, the trace wavenumbers, k1 and k2, being the wavenumber components in the x1 and x2 directions, must both satisfy Equation 2.3. Modes are then described by number pairs (n1,n2), rather than by single integers, and are most easily shown as points on a two-dimensional modal lattice, as in Figure 2.2.

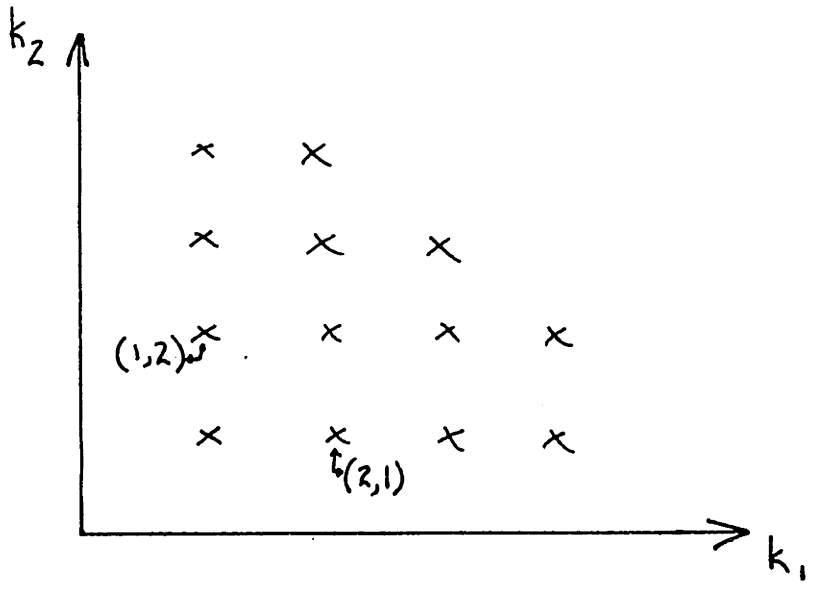

FIGURE 2.2 - Modal Lattice for Two-Dimensional Resonances

The greater the distance from the origin of the lattice that a

point is located, the higher that mode's resonant frequency. As frequency is increased, modes on the lattice do not appear in a regular pattern, especially if the structure is irregularly shaped; therefore the modal spacing for a two-dimensional structure is not constant.

The trend toward increasing modal spacing inherent in the one-dimensional dispersive system is counteracted in the plate by the fact that the number of modes allowable in a plate of dimensions LxL at a frequency ω is the square of the number of modes allowable in a beam of length L at the same frequency. Therefore as frequency increases in a two-dimensional system, the number of allowable modes increases rapidly. The net effect is that, as frequency is increased, the average modal spacing is constant even though the actual spacing is irregular. It is often more convenient to refer to the reciprocal of average modal spacing, known as the modal density, where

$\eta(\omega)$ = number of modes / frequency interval (2.6)

The modal density of a two-dimensional plate structure is constant and, when frequency is expressed in cyclic units, is equal to

$$\eta(f) = A / (4 \times pi \times \chi \times c) \qquad (2.7)$$

where A is the surface area of the plate.

2.3 STRUCTURAL TRANSFER FUNCTIONS

In a transfer function measurement, two points on a structure are considered, a source and an observer. The two-point transfer function is used to acquire magnitude and

phase information for diagnostic purposes.

2.3.1 Resonances And Antiresonances

In a simple system excited at a resonant frequency, vibration of relatively large amplitude will occur throughout the structure. This is because the energy from the input force is readily stored in vibrational modes, so the magnitude of the response at any observation point will greatly exceed that of the input. Therefore, structural resonances can be identified by locating the maxima of the transfer function magnitude. If resonant vibration cannot occur at the excitation frequency, then the response vibration will be small. The condition known as antiresonance, where the magnitude of the response is very much smaller than that of the input, is easy to visualize in a one-dimensional system. It occurs when the observation location is at a nodal point, a point of zero vibration, of the structure. This condition is presented schematically in Figure 2.3.

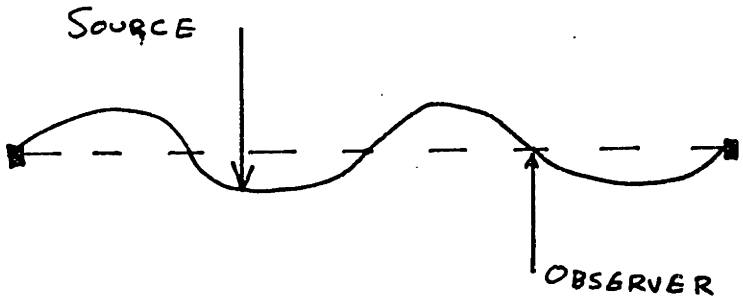

FIGURE 2.3 - One-Dimensional Antiresonance

Antiresonances of a transfer function are very sensitive to the locations of the source and the observer.

The phase of a one-dimensional transfer function is easy to determine, as the phase difference between source and observer should be a simple function of distance and wavenumber,

$$\phi = k\ (xo-xs) \qquad (2.8)$$

known as the propagation phase. Here xo and xs indicate the locations of the observer and the source.

The behavior of a two-dimensional system is more complicated since resonances do not occur in a regularly defined pattern and since antiresonances are difficult to predict analytically. Phase does not change at the same rate as one-dimensional propagation phase, since the nodes of a structure do not move in as orderly a fashion as in one dimension. In fact, experimental evidence shows that phase increases much more rapidly with frequency than propagation theory would suggest. A closer examination of transfer function properties can shed light on this paradox.

2.3.2 Poles And Zeros Of Transfer Functions

A common method used in dynamic systems analysis for representing a transfer function is a polynomial model in the frequency domain,

$$H(\omega) = A\ \frac{(\omega-\omega_a)(\omega-\omega_b)\cdots}{(\omega-\omega_1)(\omega-\omega_2)\cdots} \qquad (2.9)$$

where the roots of the numerator represent zeros of the function, frequencies for which the function equals zero, and the roots of the denominator represent poles, frequencies for which the function approaches infinity. The poles are

resonant frequencies, and the zeros are antiresonances of the transfer function.

Poles and zeros can be plotted in the complex frequency plane, as shown in Figure 2.4, where poles are represented by x's and zeros by o's.

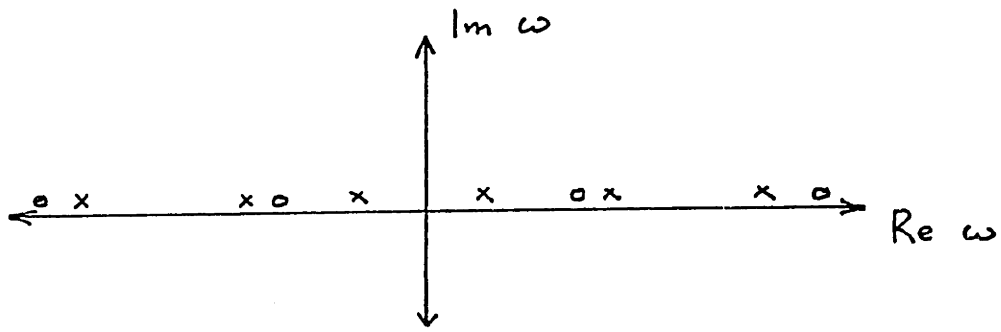

FIGURE 2.4 - Poles and Zeros in the Complex Frequency Plane

It is necessary to define frequency with real and imaginary components due to the complex frequency dependence of the Fourier Transform relationship, as in Equation 1.5. Locations of poles in the frequency plane (analogous to the "s-plane" often used in the analysis of Laplace Transforms) are restricted by the requirement that physical systems obey causality and stability. The distance of a pole above the real frequency axis is proportional to the damping inherent in that resonant mode. Therefore, a pole cannot have a negative imaginary part since negative damping would imply an unstable system. Damping ratios in a metal structure tend to be very

small, on the order of 10^{-3}, so poles tend to be very close to the real axis. There is no comparable physical restriction regarding the sign of the imaginary part of a zero; however, it is theorized that zeros have positive imaginary parts, thus satisfying the minimum phase condition. This is a topic of current research addressed in Chapter 6.

2.3.3 Determination Of Magnitude And Phase

If the locations of all zeros and poles are known for a given transfer function, then the value of the function can be computed at every real frequency value. The value of the complex function is represented by a magnitude and a phase, which are most easily determined by the analysis of phasors, or vectors in the complex plane.

The magnitude of the function given in Equation 2.9 is equal to the product of the phasor lengths from all the zeros to the frequency of interest divided by the product of the corresponding pole phasor lengths. Phasors are diagrammed in Figure 2.5.

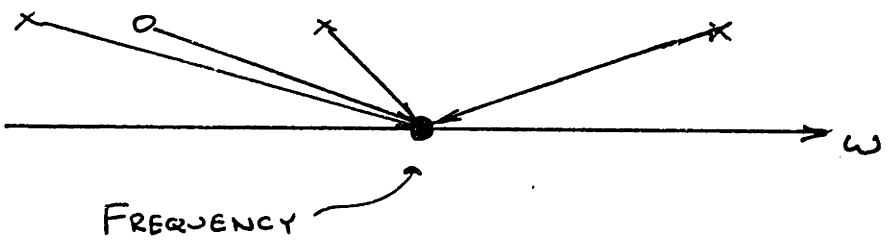

FIGURE 2.5 (a) - Phasors in the Complex Frequency Plane

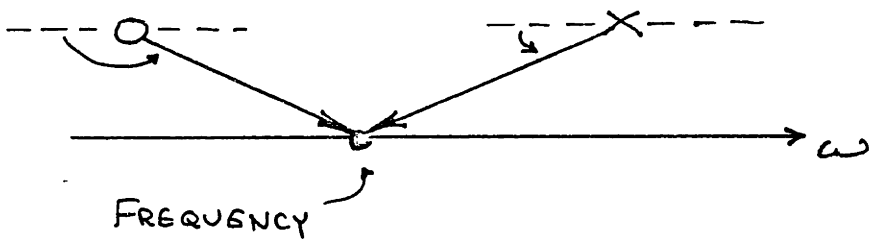

FIGURE 2.5 (b) - Phasors in the Complex Frequency Plane

Therefore if the test frequency is very near a pole, there will be a very small factor, arising from a very short phasor, in the denominator, making the value of the function very large. Conversely, if the test frequency is very near a zero, the small factor in the numerator will make the function very small.

Phase is computed by determining the sum of the angles of the phasors from the zeros to the test frequency and subtracting the sum of the angles of the phasors from the poles, also shown in Figure 2.5. Since poles and zeros are generally very close to the real axis, their contributions to the phase of the system tend to be approximately equal to +/-pi. When the test frequency passes a pole, the net phase decreases by pi and when the frequency passes a zero (above the real axis), phase is increased by pi. In this manner, the unwrapped phase can be calculated by determining how many poles and zeros occur between the origin and the frequency of interest. Assuming the phase equals zero at zero frequency,

the phase at any frequency should be

$$\phi = -(Np-Nz) \times pi \qquad (2.10)$$

where Np and Nz are the numbers of poles and zeros that exist up to that frequency.

2.3.4 The Occurence Of Zeros

As indicated before, the number of poles, equal to the number of modes, up to a given frequency can be determined from the modal density of the structure. However, since the number of zeros is not known from any physical measurements, the phase cannot be predicted from these formulas alone. To understand how zeros occur in a structural system, it is helpful to expand the transfer function polynomial in terms of partial fractions. The function is then a modal summation, with each term corresponding to a resonance;

$$H(\omega) = A \sum_{M} \frac{\Psi_M(x_s) \cdot \Psi_M(x_o)}{\omega^2 - \omega_M^2} \qquad (2.11)$$

The factors in the numerator represent normalized modeshapes.

Each term in the expansion has a shape as in Figure 2.6, although the sign of each term can be positive or negative. To simplify the analysis, the summation at any frequency can be represented by the two dominant terms, those corresponding to the nearest poles, and a single remainder term representing the sum of all other modal terms. If the remainder term is assumed to be negligibly small, then if two adjacent terms have the same sign they will add to zero at some point between the two resonances. If they have opposite signs, they will not add to zero. These two conditions are shown in Figure 2.6.

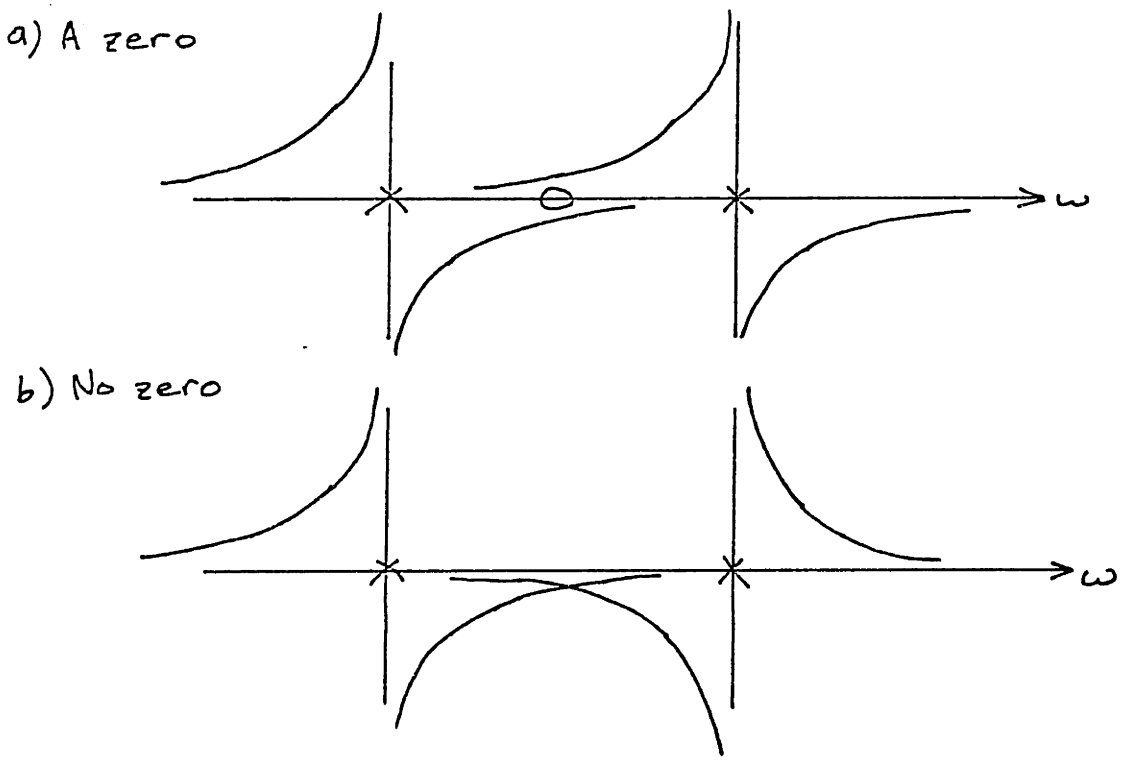

FIGURE 2.6 - The Occurence of a Zero

Unless the remainder term is large compared to the two dominant modal terms, then the existence of a remainder will only serve to shift the location of the zero slightly, but will not effect the existence of the zero. It can be shown that either sign is equally likely for any term in the sum, but that there is no pattern in the sign changes. Therefore a sign change should occur on average between every other pair of resonances, so the density of zeros should be half that of poles. Up to any frequency, the net phase should be

$$\phi = -(Np / 2) \times pi \qquad (2.12)$$

in a two-dimensional structural system.

CHAPTER 3

EXPERIMENTAL TECHNIQUE

Transfer functions have been measured on partially completed diesel engines on two occasions, first in 1983 and then in March 1985. Both experiments were conducted at the manufacturing facility of the Cummins Engine Company in Columbus, Indiana. The results of the first experiment were originally reported in the thesis of Murville [3]. Those data are reviewed and the results from the second set of experiments are presented in this thesis.

3.1 THE INITIAL EXPERIMENT (1983)

In the original set of experiments, the test apparatus was set up beside an engine assembly line at a point where the engines were nearly complete. The engines being assembled were large eight-cylinder diesels designed for trucks or agricultural equipment. As each engine passed on the line, a transfer function was measured and recorded using a Hewlett-Packard 5423A two-channel spectrum analyzer. The 128 engines analyzed were of three types, distinguished by the

size of the cams and the oil pans. In addition, one engine type was tested in two different manners. The engines could therefore be divided into four ensembles, as follows:

BIGCAM large cams, accelerometers attached with wax
43 engines

BCTAPE large cams, accelerometers attached with tape
23 engines

SMCAM small cams, small oil pans
28 engines

SMCAMO small cams, large oil pans
34 engines

The engines were not operating at the time of the test. The force input was provided by a mechanical shaker, and the vibration output at another point on the structure was measured by an accelerometer. A sample transfer function is shown in Figure 3.1. Magnitude was determined, in decibel measure, by computing

$$|H(\omega)| = 10 \times \log(\sqrt{(re^2 + im^2)}) \qquad (3.1)$$

Here, re represents the real component of the transfer function, and im represents the imaginary part. The dimensions of magnitude are accelerance, or acceleration divided by force. Phase, in radians, is determined by

$$\phi = \arctan (im / re) \qquad (3.2)$$

and was computed using the unwrapping algorithm.

One can easily identify the resonances and antiresonances from the magnitude spectrum of the transfer function. Also one notices the continually decreasing value of phase. Measurements were performed from 0 to 25.6 khz. This broad range was chosen because it was desired to include high

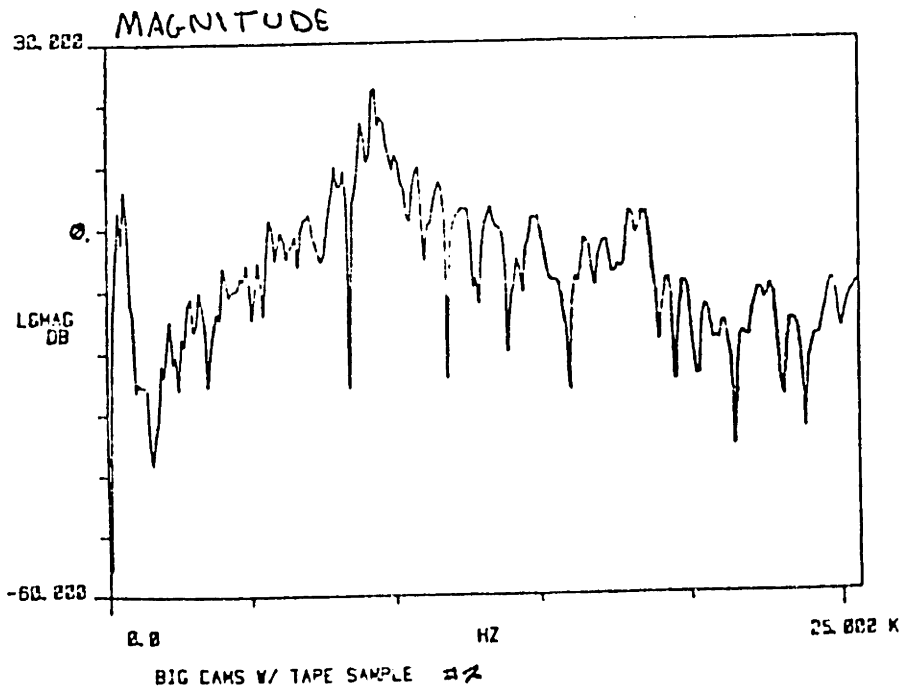

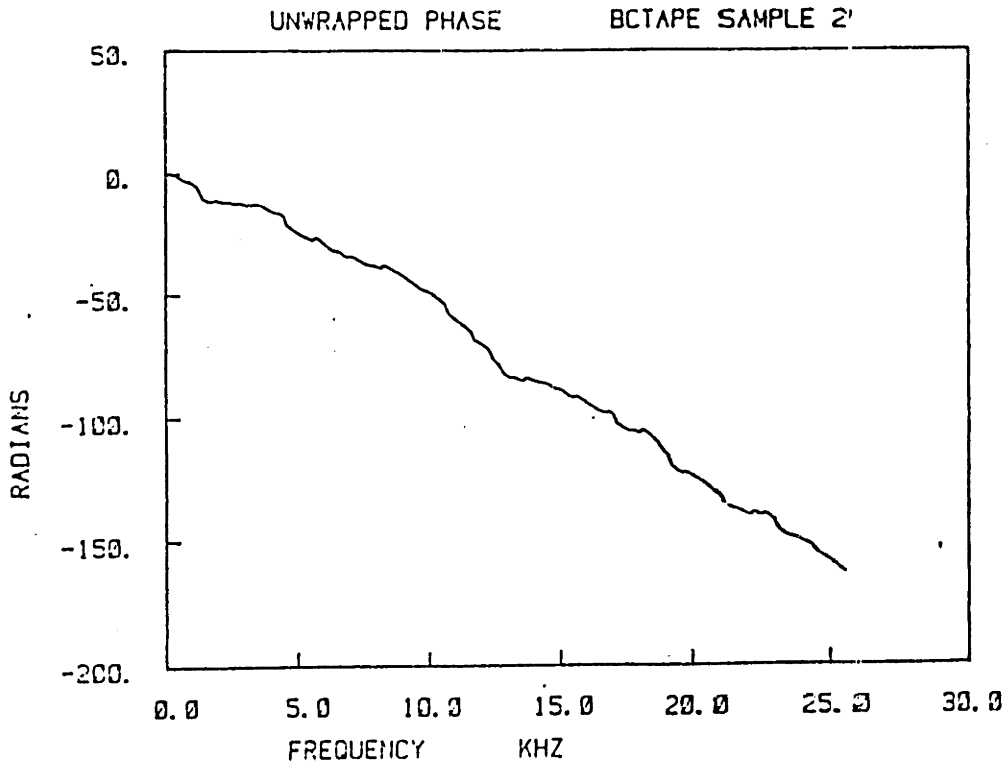

FIGURE 3.1 - Sample Engine Transfer Function (1983)

frequency information, often valuable in signal reconstruction. However, since the spectrum analyzer only records 256 frequency lines in its Fast Fourier Transform, data points were only recorded every 100 Hz.

The variability of these transfer functions was assessed as part of Murville's work. For each ensemble of engines, the mean and standard deviation of both log magnitude and phase were computed at every frequency point. It was found that the standard deviations were quite high, especially for the phase spectra. This was not encouraging, since the engines in each ensemble were as identical to each other as any machines can reasonably be. High phase variability suggests that inverse filtering cannot be successfully applied to a group of similar machines.

The major reason suspected for the high variability was the large line spacing. Phase spectra tend to change much more rapidly than every 100 Hz, so with this spacing, the unwrapping algorithm misses some of the phase features. If the resolution is not sufficient to track the changes in the phase derivative, then the phase curves will not be accurate.

3.2 THE SECOND EXPERIMENT (1985)

The second set of experiments was designed to perform similar measurements, but with increased frequency resolution and with simpler structures. The items analyzed were to be bare engine castings, structures even more identical than the

assembled engines. The experiment was designed to test whether the variability arose in the engine assembly process or was inherent in the structures themselves. In addition to the castings, transfer function measurement was repeated on partially assembled engines and also performed on completed engines both before and after their first test run. These data were collected to show how variability changed through the process of building and operating a machine.

The castings actually supplied for analysis were not completely bare, but had a set of bearing caps loosely fastened with assembly bolts. The castings were stacked on wooden pallets, or skids, on the shop floor. The engines analyzed in 1985 were all of the same design and were all measured at the same location on the assembly line. The completed engines were mounted on test stands on the shop floor. The pretest engines had just come off the assembly line. The posttest engines had just been operating in a test bay; therefore they were slightly warmer than the pretest engines and presumably had lubricants evenly distributed throughout the moving parts. The points for force input and acceleration output were arbitrarily chosen, but were kept the same for all structures measured. The major ensembles of the 1985 experiment are as follows:

CASTINGS	45 castings with bearing caps
ENGINES	43 engines on the assembly line
PRETEST	12 assembled engines before first operation
POSTTEST	12 assembled engines after first operation

The new experiment was conducted using a different analyzer, a Bruel & Kjaer Model 2032 Dual Channel Analyzer. This instrument has the capacity to store 801 lines of frequency information. The transfer functions were only measured from 0 to 3.2 khz, improving the frequency spacing to 4 Hz. The high frequencies studied in the first experiment were ignored since actual inverse filtering was not to be performed, and their inclusion would have only served to degrade the resolution.

The force input was from a Bruel & Kjaer Model 4810 one-pound mechanical shaker. It was excited with pseudo-random noise supplied from the signal generator of the analyzer. The noise signal was amplified via a Macintosh power amplifier. Attached to the shaker was a Wilcoxon F9 impedance head which provided the input force signal to the analyzer. The shaker was hand-held in use. The force spectrum alone was measured before any transfer functions were attempted. An MXR 31-band equalizer was used to modify the input until a flat force spectrum was obtained.

The accelerometer used was a BBN model, attached to the structure magnetically. The signals from both the accelerometer and impedance head were low-pass filtered before being passed to the analyzer. Although the analyzer is equipped with internal input filters and preamplifiers, the extra filtering was performed to guard against aliasing. Aliasing occurs when a signal frequency is higher than the Nyquist frequency, equal to one-half the sampling frequency of

the analyzer. If aliasing exists, the spurious high frequency signal components are not properly measured in the Fourier Transform. Instead, they contaminate the spectrum, taking on the 'alias' of lower frequency components.

For each transfer function, the shaker and accelerometer were held in place until the analyzer completed ten averages. The transfer function data, in the form of real and imaginary parts, were then transferred to cassette tape via a Bruel & Kjaer 7400 cassette recorder before the next transfer function was measured.

Once in the laboratory, a data transfer routine was written using a Digital Equipment PDP-11/44 computer. The real and imaginary data were passed to the computer for storage and all additional analysis. On account of some faulty cassettes, a few transfer functions could not be saved. However, this loss did not significantly degrade the sample size for any portion of the experiment.

CHAPTER 4

A REVIEW OF VARIABILITY DATA

In this chapter, the results of the transfer function measurements from both the 1983 and 1985 experiments are presented. The variability of both the magnitude and phase spectra is assessed by applying simple statistical analysis.

4.1 THE 1983 DATA

The first data, presented in Figures 4.1 through 4.4, are the mean phase and magnitude curves for the four ensembles of engines in the 1983 experiment. The curves above and below each mean curve represent variability 'envelopes,' marking the standard deviation of the data at each frequency. Standard deviation, σ, of magnitude or phase, represented here by the variable x, was computed using the formula

$$\sigma^2 = E[(x - E[x])^2] = E[x^2] - (E[x])^2 \qquad (4.1)$$

where E[] denotes the expected value of the quantity within the brackets. (For normally distributed, or Gaussian, random variables, approximately 68% of the data points lie within one standard deviation of the mean.)

The ensembles of transfer functions look quite similar in both magnitude and phase behavior. The magnitude curves all show the same general shape, and the standard deviation of magnitude in each ensemble remains approximately constant at 8 to 10 decibels across the frequency range. The mean unwrapped phase curves are all very nearly linear, with a value of approximately -160 radians at 25.6 kHz. The standard deviation of phase tends to increase with frequency, rather than remain approximately constant as in the case of magnitude. However, the deviation does not seem to increase in a strictly linear fashion, but more slowly at higher frequencies. The large cam engines, shown in Figures 4.1 and 4.2, tend to have somewhat greater variability than the small cam engines, Figures 4.3 and 4.4, as the standard deviation in the 'Bigcam' ensembles reaches about 30 radians at 25.6 kHz compared with about 20 radians in the 'Smallcam' ensembles.

An important feature of these data is revealed by comparing the mean unwrapped phase result with the theoretical prediction. By combining Equations 2.6, 2.7, and 2.12, eliminating modal density, the expected phase can be estimated from only the structure's geometry and material properties;

$$\phi = \frac{90\sqrt{3} \cdot A \cdot f}{h \cdot c} \qquad (4.2)$$

where h and A are plate thickness and area, expressed in units of feet, and f is the cyclic frequency. For a wave speed in steel of 17,000 feet per second and an estimated engine wall thickness of 0.03 feet, the engine area can be treated as the unknown variable; the value which results from this

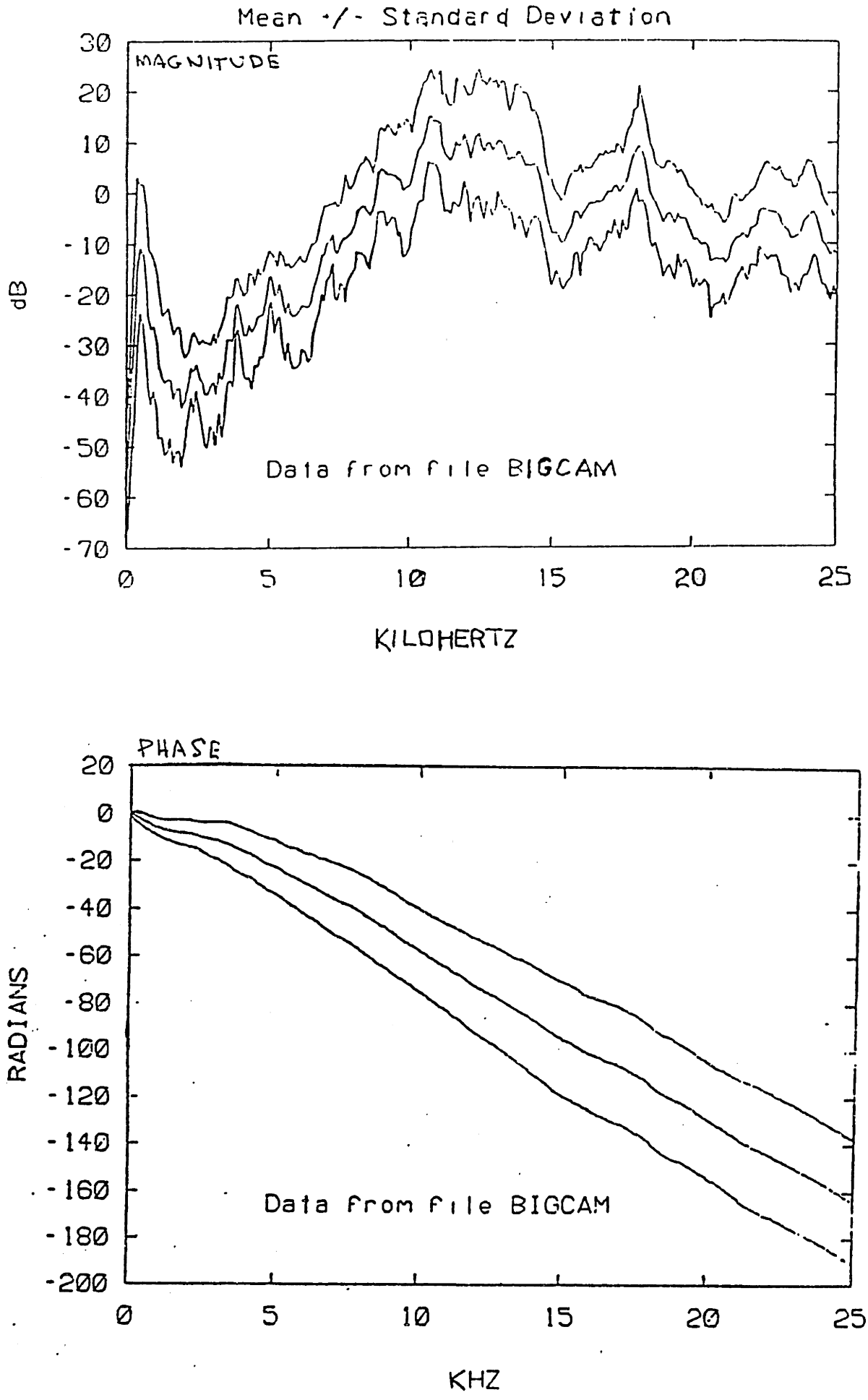

FIGURE 4.1 - Ensemble Statistics, BIGCAM Engines

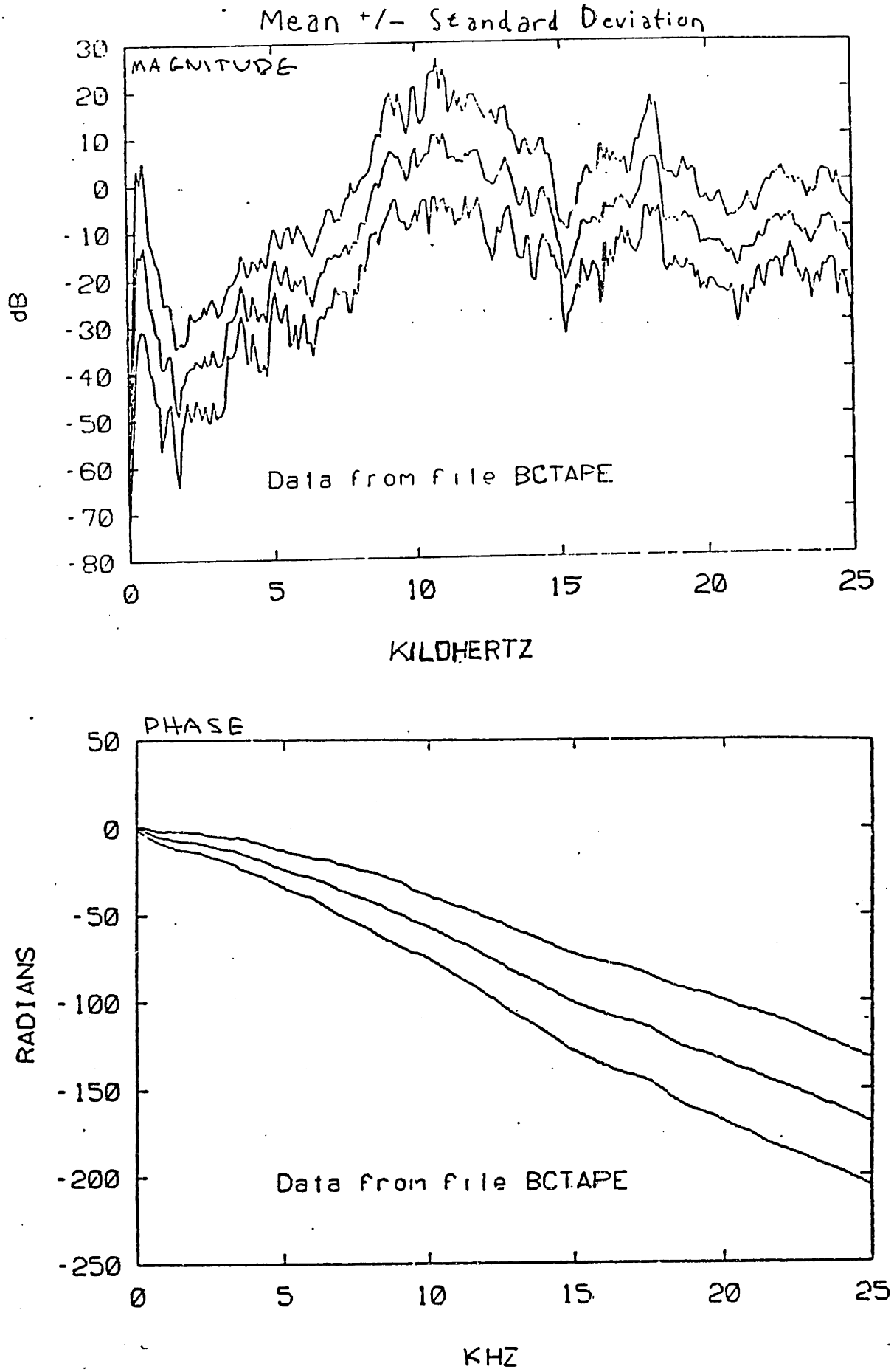

FIGURE 4.2 - Ensemble Statistics, BCTAPE Engines

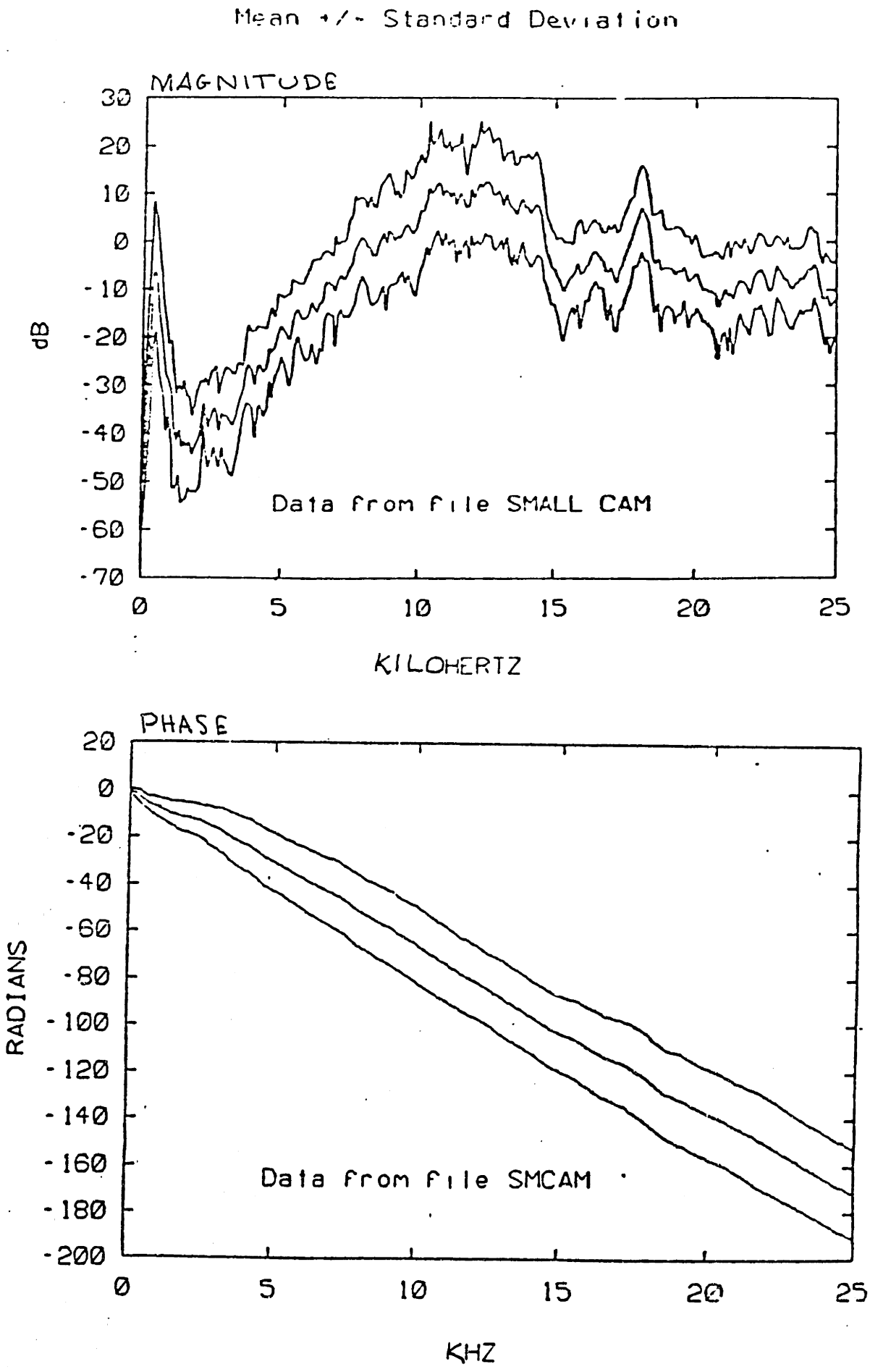

FIGURE 4.3 - Ensemble Statistics, SMCAM Engines

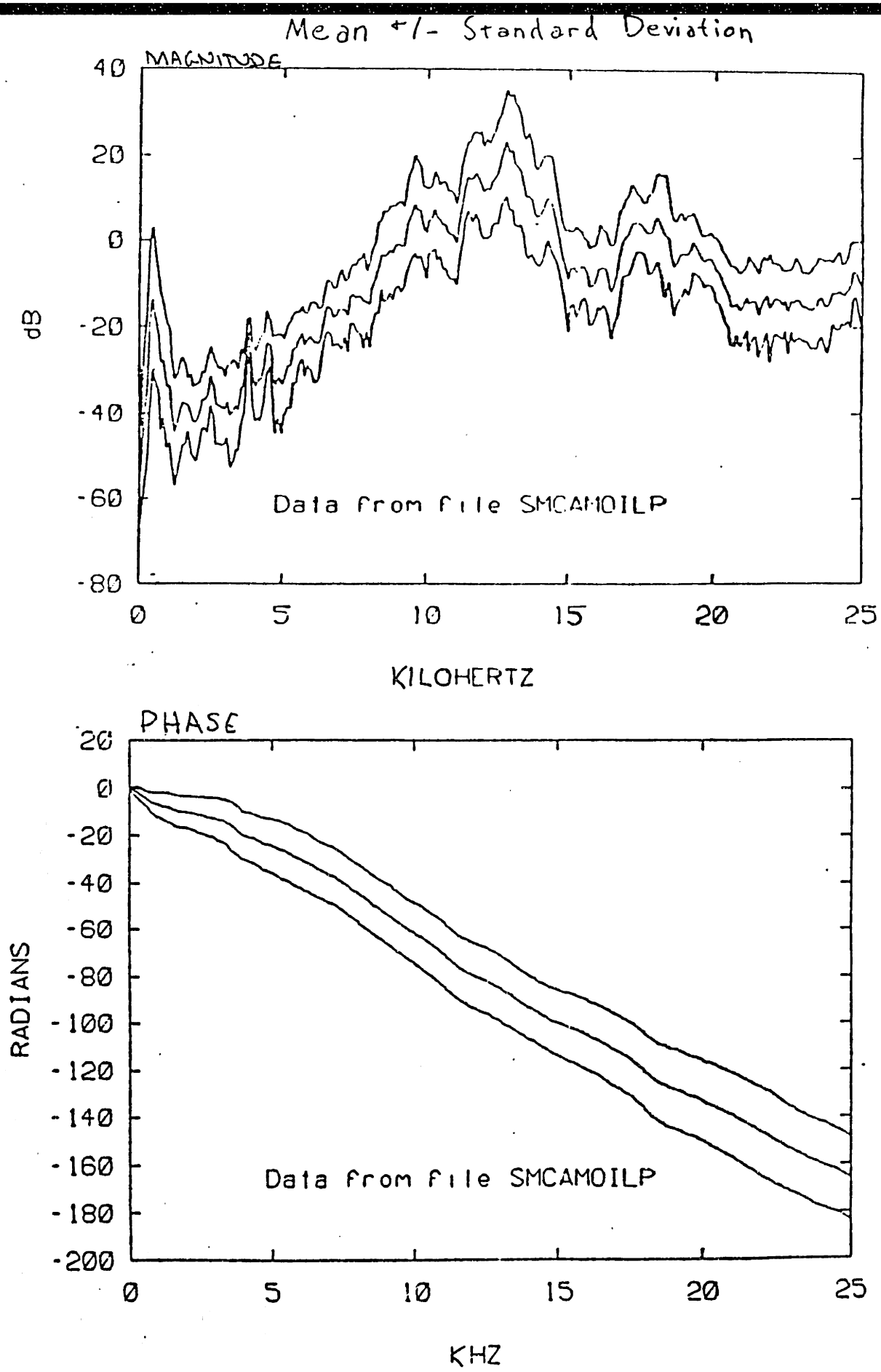

FIGURE 4.4 - Ensemble Statistics, SMCAMO Engines

calculation is a plate area of approximately 1 square foot, far too small for the structures which were tested. Therefore it seems likely that the unwrapped phase values are too small. It is suspected that the large frequency line spacing of the transfer function measurement may account for this, since the phase unwrapping algorithm depends upon good resolution with respect to modal density.

Considering the precision required in a phase spectrum, especially at high frequencies, for successful inverse filtering, the standard deviations of phase seem much too high to leave any hope for applying a general inverse filter to an ensemble of engines. The 1985 experiment was performed to learn if simpler structures and better frequency resolution would improve the results.

4.2 THE 1985 DATA

A key goal of the 1985 experiment was to improve the procedure for measuring the transfer functions. So some tests were performed to see how much variability was introduced by the measurement technique. Transfer functions on a single casting with the bearing caps removed were measured several times while introducing very slight measurement changes. Specifically, an accelerometer was fixed and five transfer functions were measured, each time shifting the location of the shaker by a centimeter or so. Then, with the shaker held still, the procedure was repeated moving the accelerometer. Mean and standard deviation results are shown in Figures 4.5

and 4.6. The variability here is somewhat smaller than for any of the large ensembles, and reflects the precision of the measurement procedure itself.

The fact that the deviation with shaker movement is slightly larger than that with accelerometer movement may result from the larger contact area of the accelerometer, a diameter of perhaps 2 centimeters compared with nearly a point contact for the shaker. The greater spatial averaging of the accelerometer may make it less sensitive to small movements. In a similar test, two different people held the shaker during different measurements. This was only tested once on each of two different castings, so no accurate standard deviation data are available. However, no significant change was noted in either transfer function as a result of this action.

In an additional test of the experimental and analytical procedure, phase unwrapping was repeated on several transfer functions to see if the performance of the algorithm could in any way affect the variability. For each transfer function examined, unwrapping was performed several times while the consistency parameters of the program, which govern the threshold of acceptable precision of the result, were varied over a wide range, yet no change was apparent in any phase curve. Therefore the unwrapping is assumed to be consistent.

Mean and standard deviation data are shown in Figures 4.7 through 4.10 for the four major ensembles of the second experiment: castings, partially assembled engines, pretest,

and posttest engines. Considering the smaller frequency range of these measurements, it is significant that the mean unwrapped phase increases faster than in the cases previously shown. Applying a typical phase value of 125 radians at 3.2 kHz in Equation 4.2, a plate area of 7.5 square feet is obtained, a much more reasonable estimate of the actual engine size. This suggests that the increased resolution substantially improved the accuracy of the unwrapped phase. The mean phase values for the three ensembles of assembled structures are quite similar, but considerably smaller than that of the simple castings, a rather surprising fact that is considered further in Chapter 6.

The phase standard deviation values for all ensembles display the same increasing trend as in the data previously shown in Figures 4.1 through 4.4. It was expected that the castings would show considerably more uniformity than any of the groups of engines, but in fact the standard deviations of castings and of engines on the line are quite similar, reaching about 18 radians at 3.2 kHz. The pretest engines show somewhat greater variability, but surprisingly the posttest engines have a standard deviation of only about 10 radians at 3.2 kHz.

It is difficult to interpret whether or not the amount of variability is less than in the 1983 data. As a function of unwrapped phase, the standard deviation is lower, about 18 radians in 1985 compared to 20 to 30 radians in 1983, when the total phase delay in both cases is approximately 150 radians. This is especially good since so many more data points are

included in the 1985 experiment, 800 per transfer function compared to 256. However, if the standard deviation is viewed as a function of frequency, then it is higher in the 1985 data, 18 radians at only 3.2 kHz compared to 20 to 30 radians all the way to 25.6 kHz.

There is no significant difference among the ensembles in the magnitude standard deviation results; all are approximately constant around 7 dB across the frequency range. There seems to be no direct correlation between magnitude and phase variability. This is unfortunate since it would be convenient to be able to quickly assess the precision of unwrapped phase data from an examination of only the magnitude. Magnitude data can be examined at the experimental site, whereas access to a computer is required for phase to be unwrapped.

A group of four transfer functions of castings which had the bearing caps removed was compared to four transfer functions of castings with bearing caps. This was done to learn if the loosely fitting bearing caps substantially degraded the uniformity of the transfer function data. These data, shown in Figures 4.11 and 4.12, are puzzling due to the mean phase behavior. The castings without caps show a net phase of about 190 radians, consistent with the trend of simpler structures displaying greater phase advance, apparent in the four major ensembles. However, the castings with caps, similar to those tested in the large ensemble of castings, show much less net phase than either the large ensemble or the group

without caps, only about 120 radians. It is also somewhat surprising that the simpler structures, those without caps, show greater variability than those with caps.

Finally, a test was made to measure variability when no two transfer functions were the same. On a sample casting, without bearing caps, five shaker locations and five accelerometer locations were chosen arbitrarily. Using these points, 25 different transfer functions were measured. These data are shown in Figure 4.13, and, as expected, the standard deviation was quite high.

As shaker or accelerometer location is changed, the resonant behavior of the casting vibration does not change, since, at resonance, the entire structure is greatly excited. However, the behavior around antiresonances does change, since antiresonances are very sensitive to source and observation points. Therefore in these data the frequencies of the poles should be the same throughout the ensemble, but the frequencies of the zeros should be different in each sample. The peaks in magnitude are expected to remain well defined while the valleys should be difficult to identify. According to Equation 2.12, the net phase should be the same as in the case of identical transfer functions, since the density of zeros should be unchanged if the density of poles is unchanged. The standard deviation of phase should be greater in the case of spatial averaging because the phase steps of +pi, arising from the zeros, occur at different frequencies in each sample.

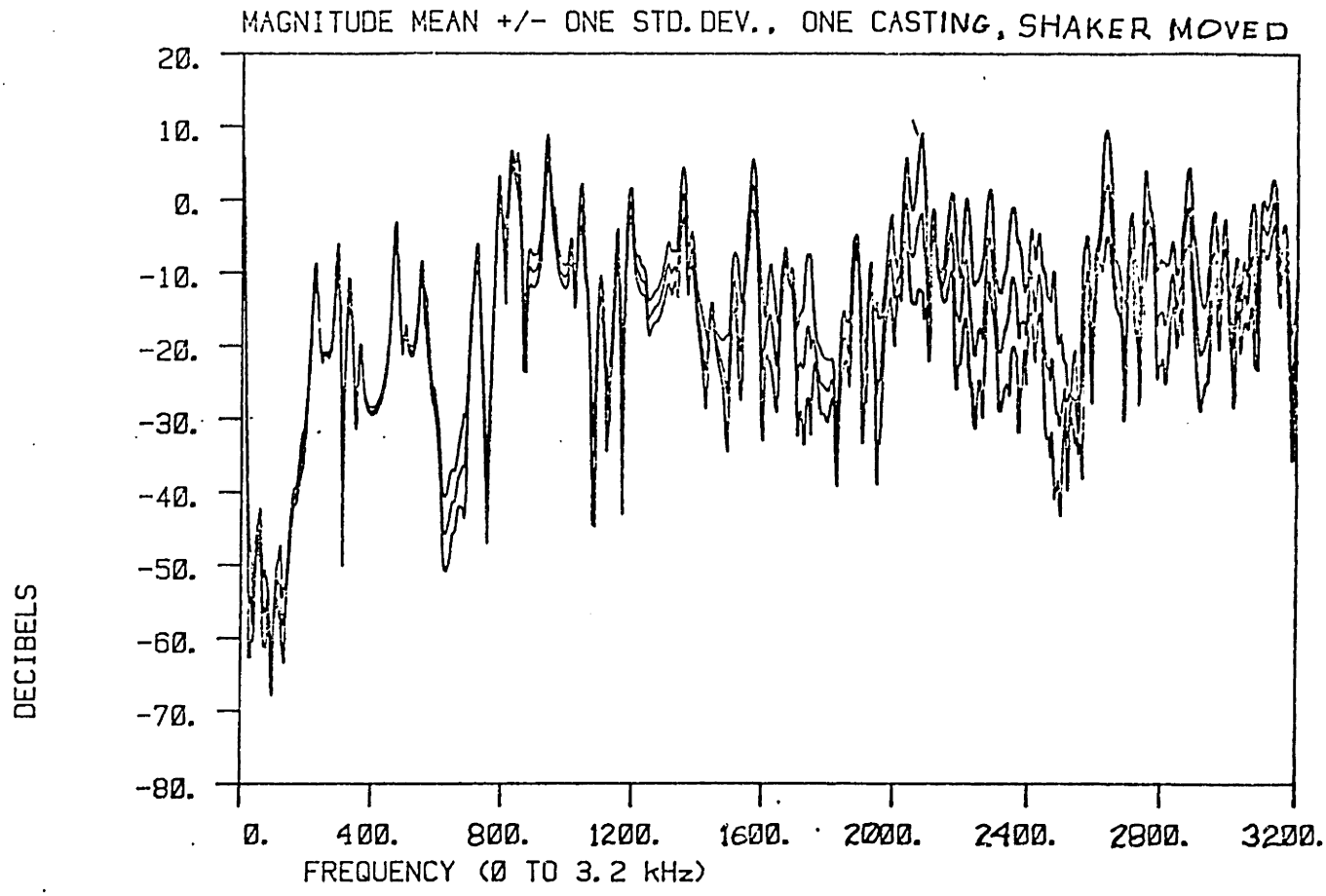
MAGNITUDE MEAN +/- ONE STD. DEV., ONE CASTING, SHAKER MOVED
20.
10.
0.
-10.
-20.
-30.
-40.
-50.
-60.
-70.
-80.
DECIBELS
0.
400.
800.
1200.
1600.
2000.
2400.
2800.
3200.
FREQUENCY (0 TO 3.2 kHz)

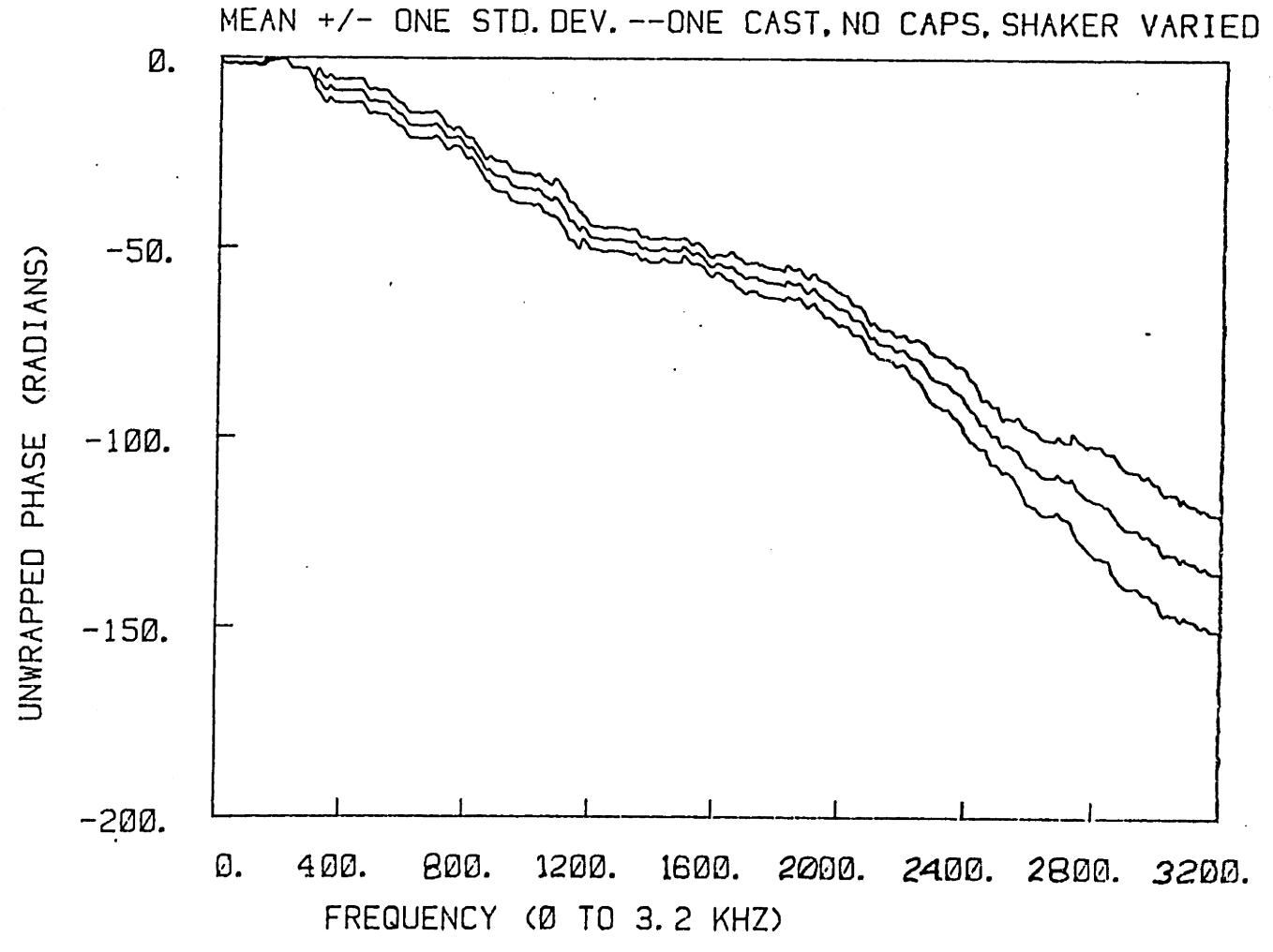
MEAN +/- ONE STD. DEV. --ONE CAST, NO CAPS, SHAKER VARIED
0.
-50.
-100.
-150.
-200.
UNWRAPPED PHASE (RADIANS)
0.
400.
800.
1200.
1600.
2000.
2400.
2800.
3200.
FREQUENCY (0 TO 3.2 KHZ)

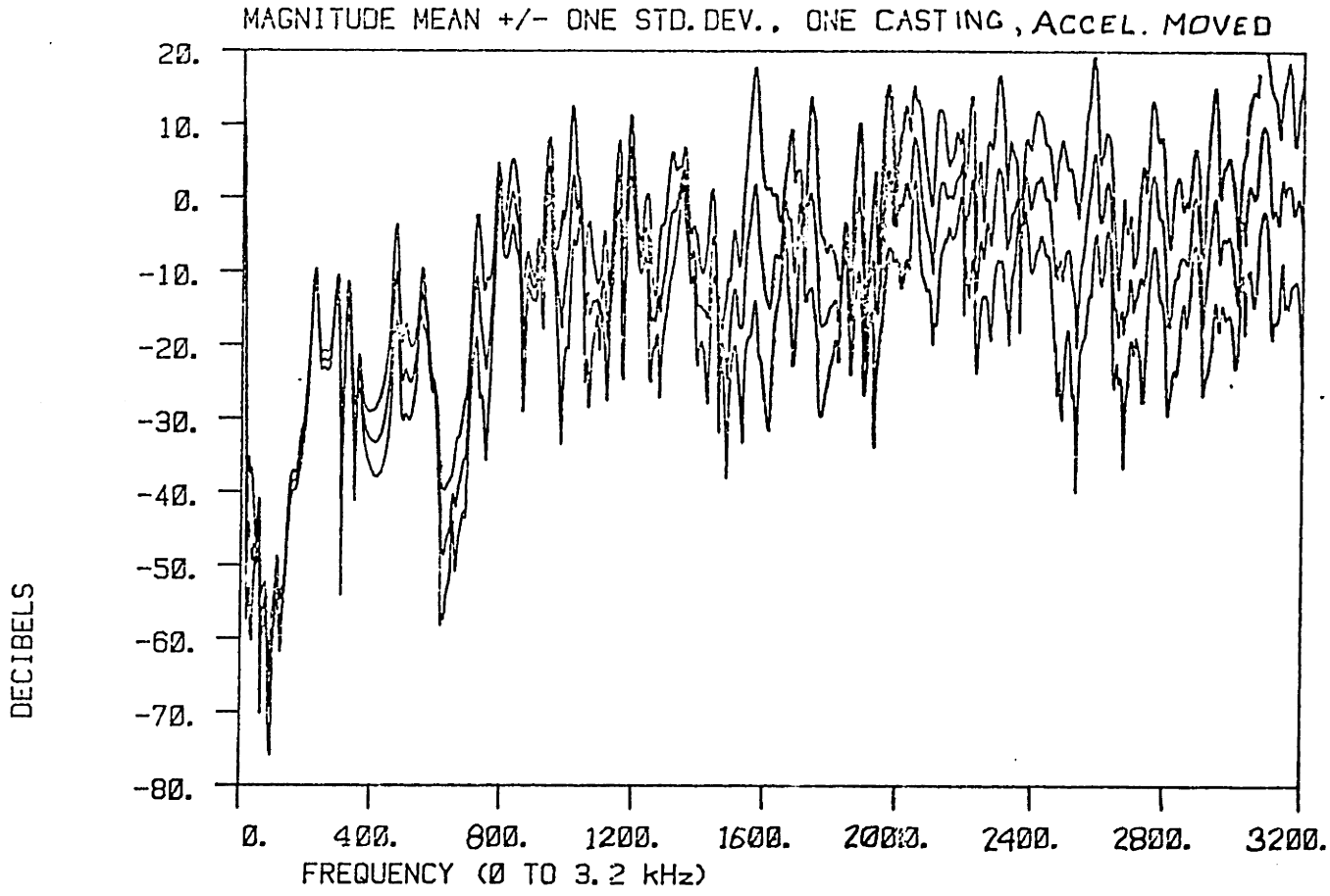
MAGNITUDE MEAN +/- ONE STD. DEV., ONE CASTING, ACCEL. MOVED
DECIBELS
20.
10.
0.
-10.
-20.
-30.
-40.
-50.
-60.
-70.
-80.
0.
400.
800.
1200.
1600.
2000.
2400.
2800.
3200.
FREQUENCY (0 TO 3.2 kHz)

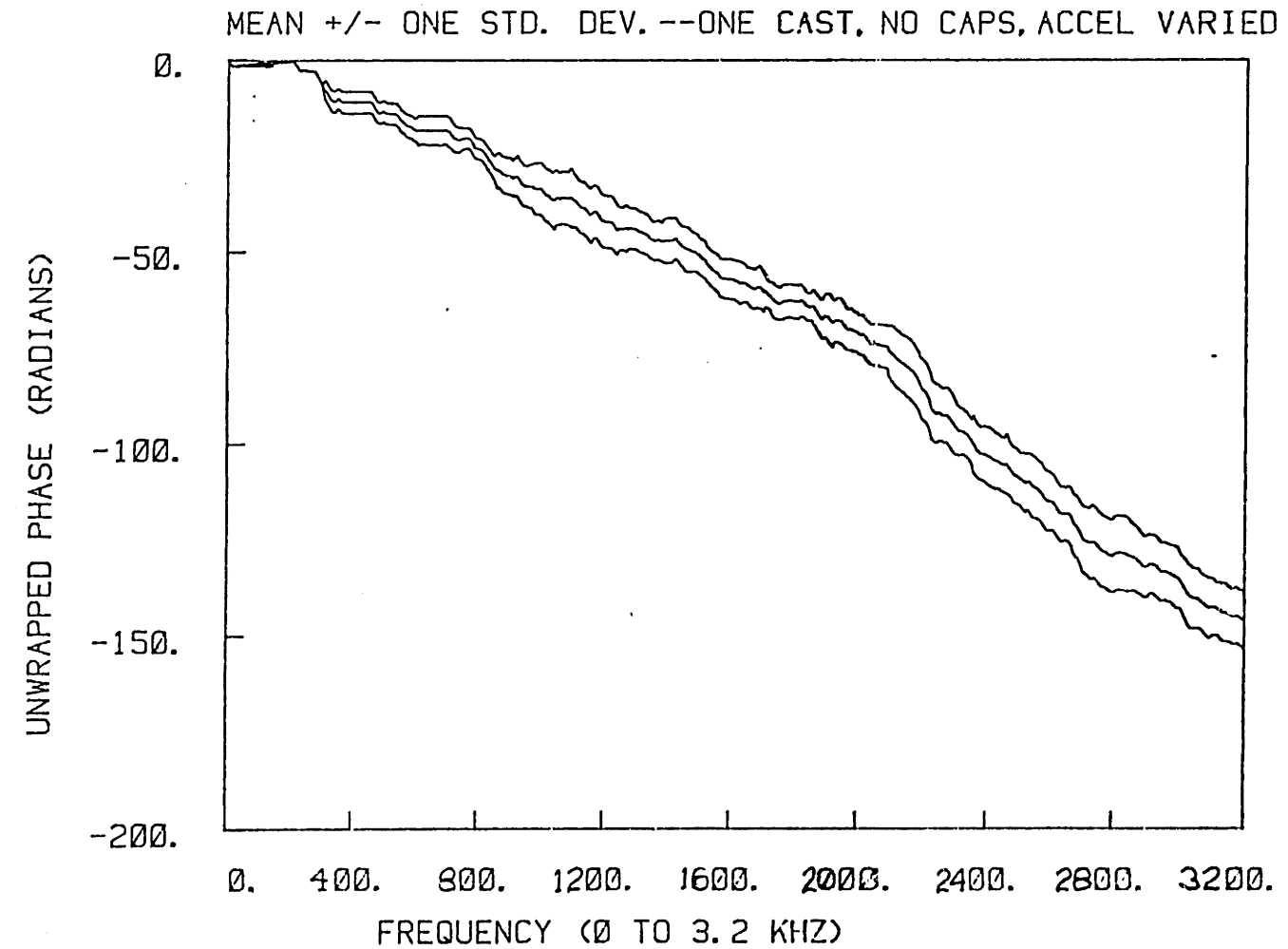
MEAN +/- ONE STD. DEV. --ONE CAST, NO CAPS, ACCEL VARIED
UNWRAPPED PHASE (RADIANS)
0.
-50.
-100.
-150.
-200.
0.
400.
800.
1200.
1600.
2000.
2400.
2800.
3200.
FREQUENCY (0 TO 3.2 KHZ)

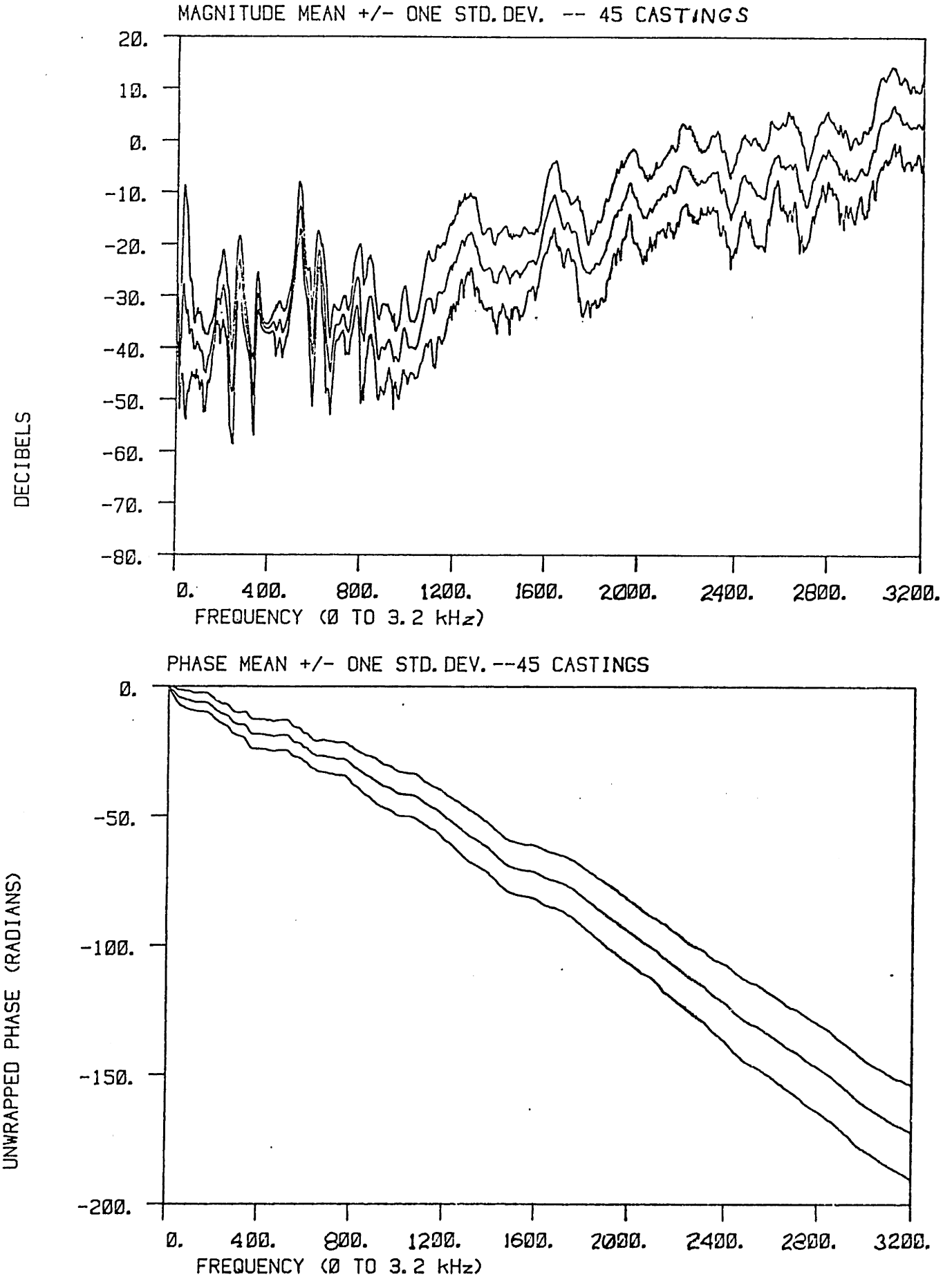

FIGURE 4.7 - Ensemble Statistics, Castings

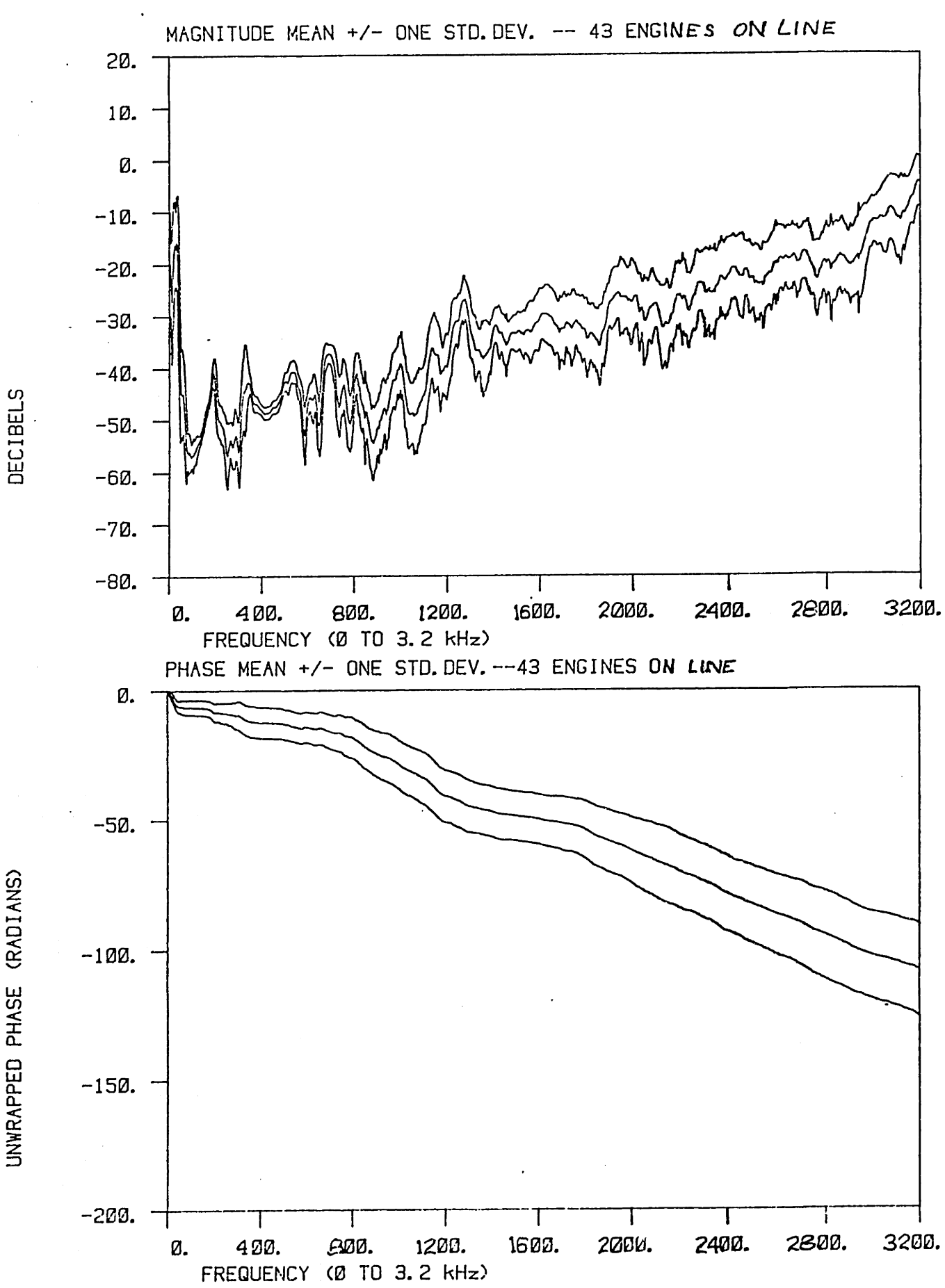

FIGURE 4.8 - Ensemble Statistics, Engines on Line

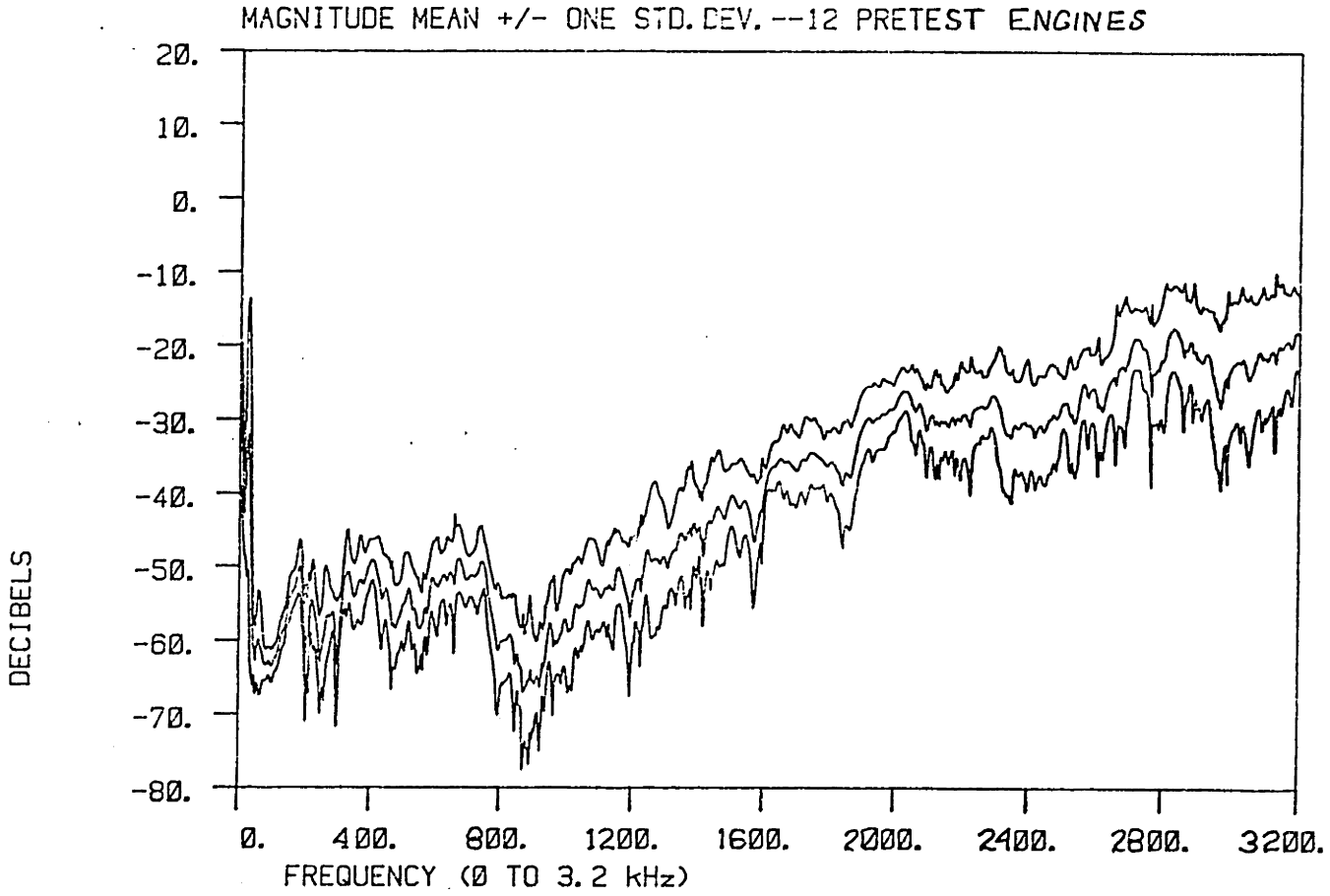

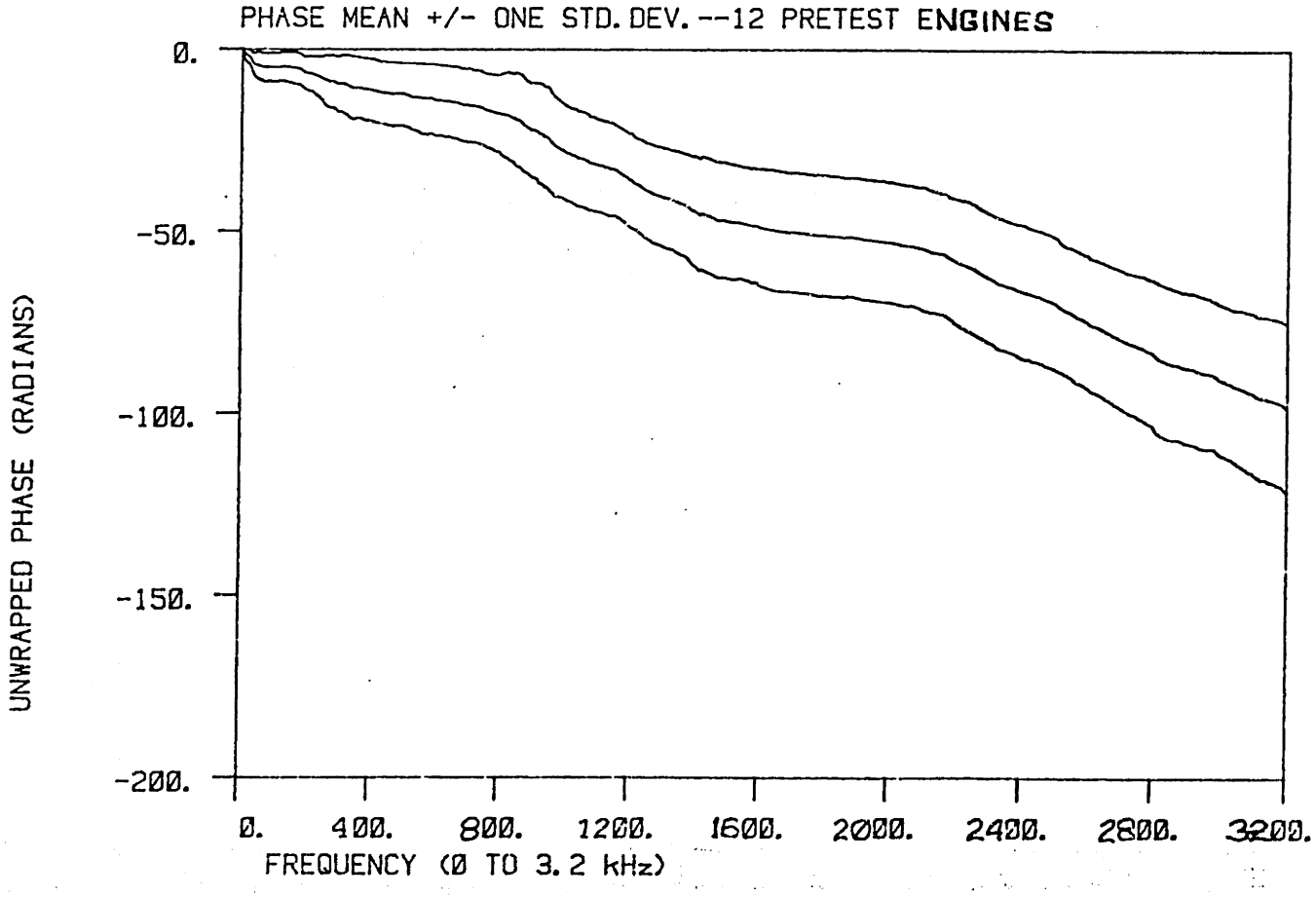

FIGURE 4.9 - Ensemble Statistics, Pretest Engines

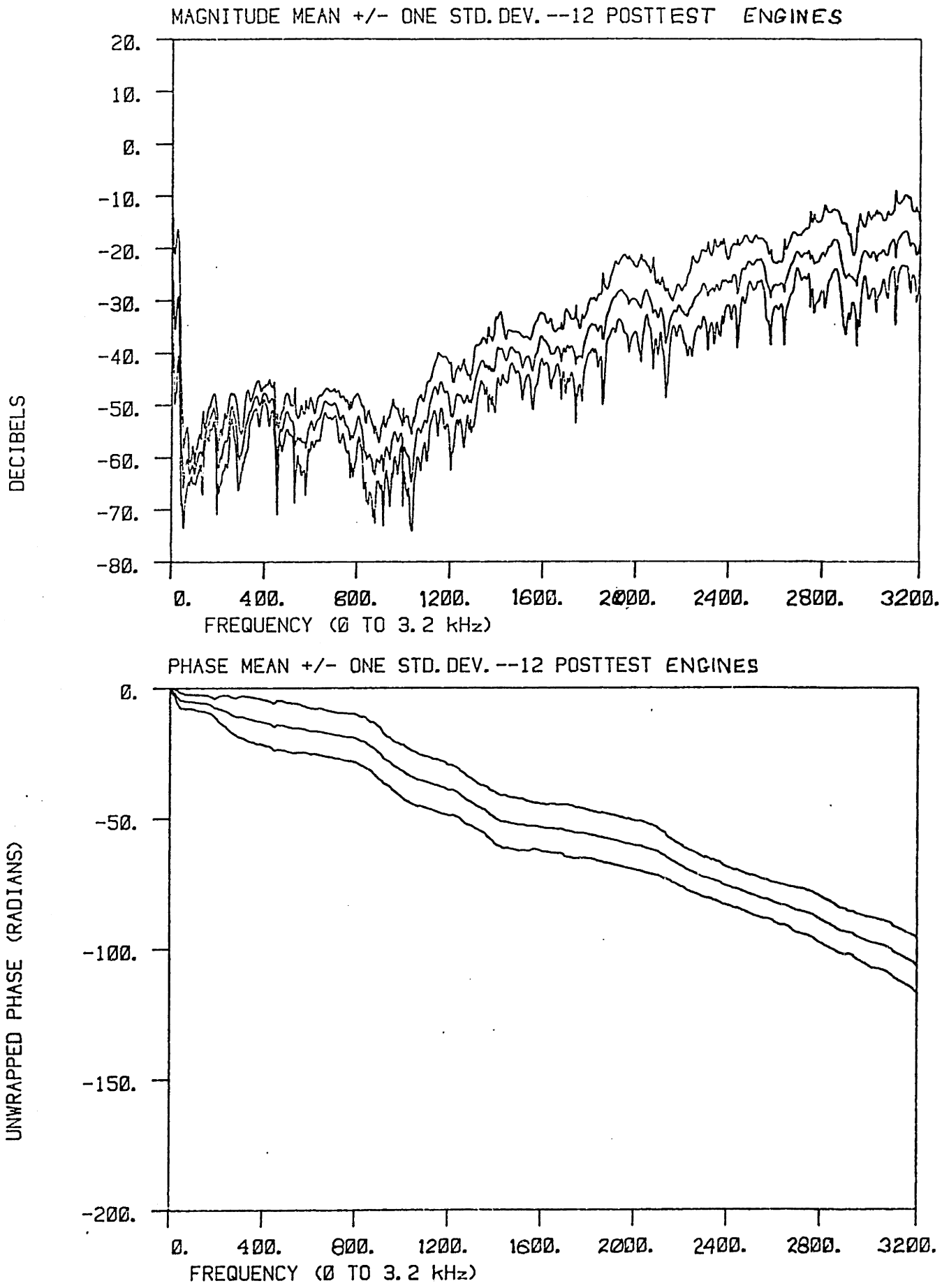

FIGURE 4.10 - Ensemble Statistics, Posttest Engines

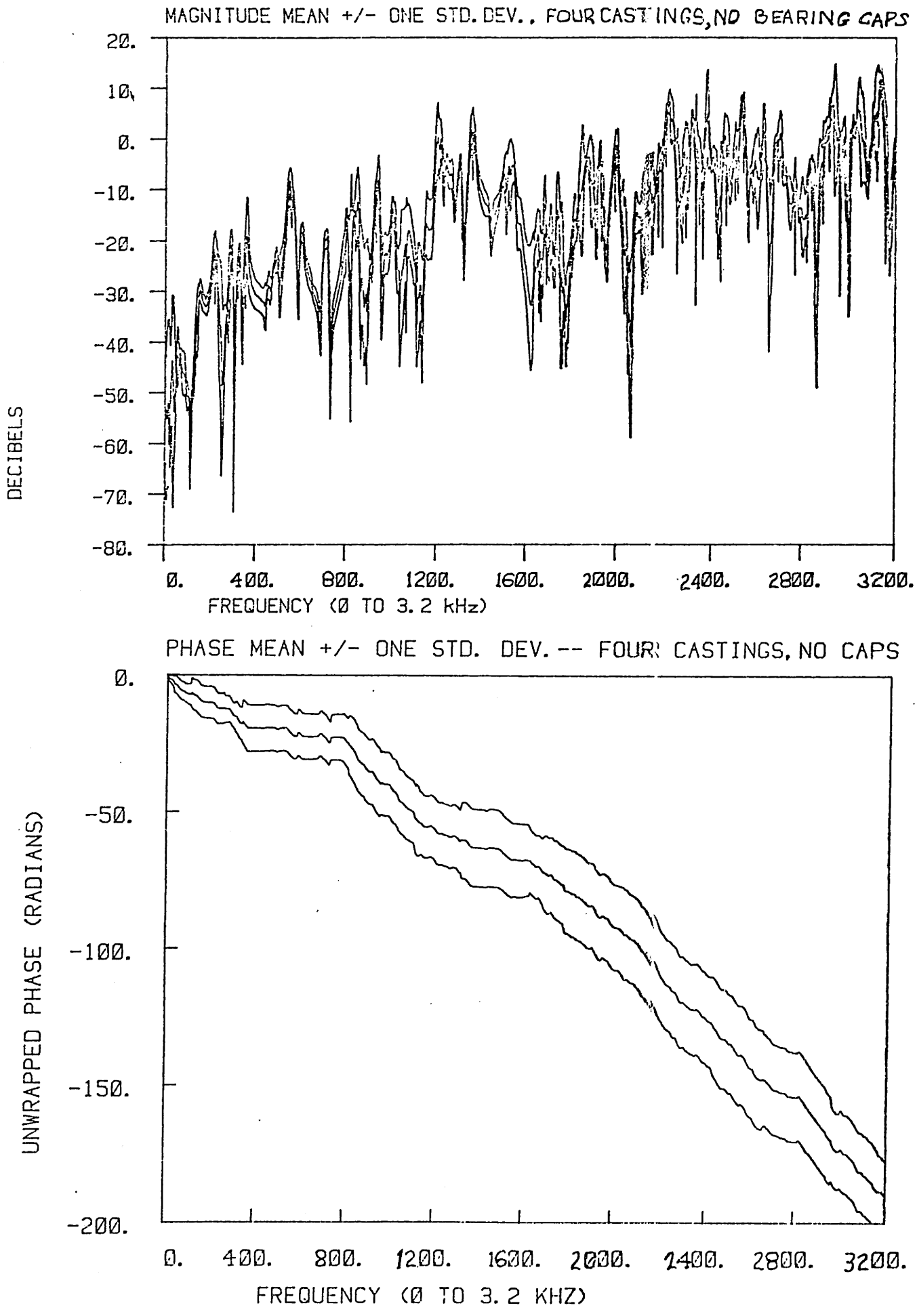

FIGURE 4.11 - Ensemble Statistics, Four Transfer Functions, Castings Without Bearing Caps

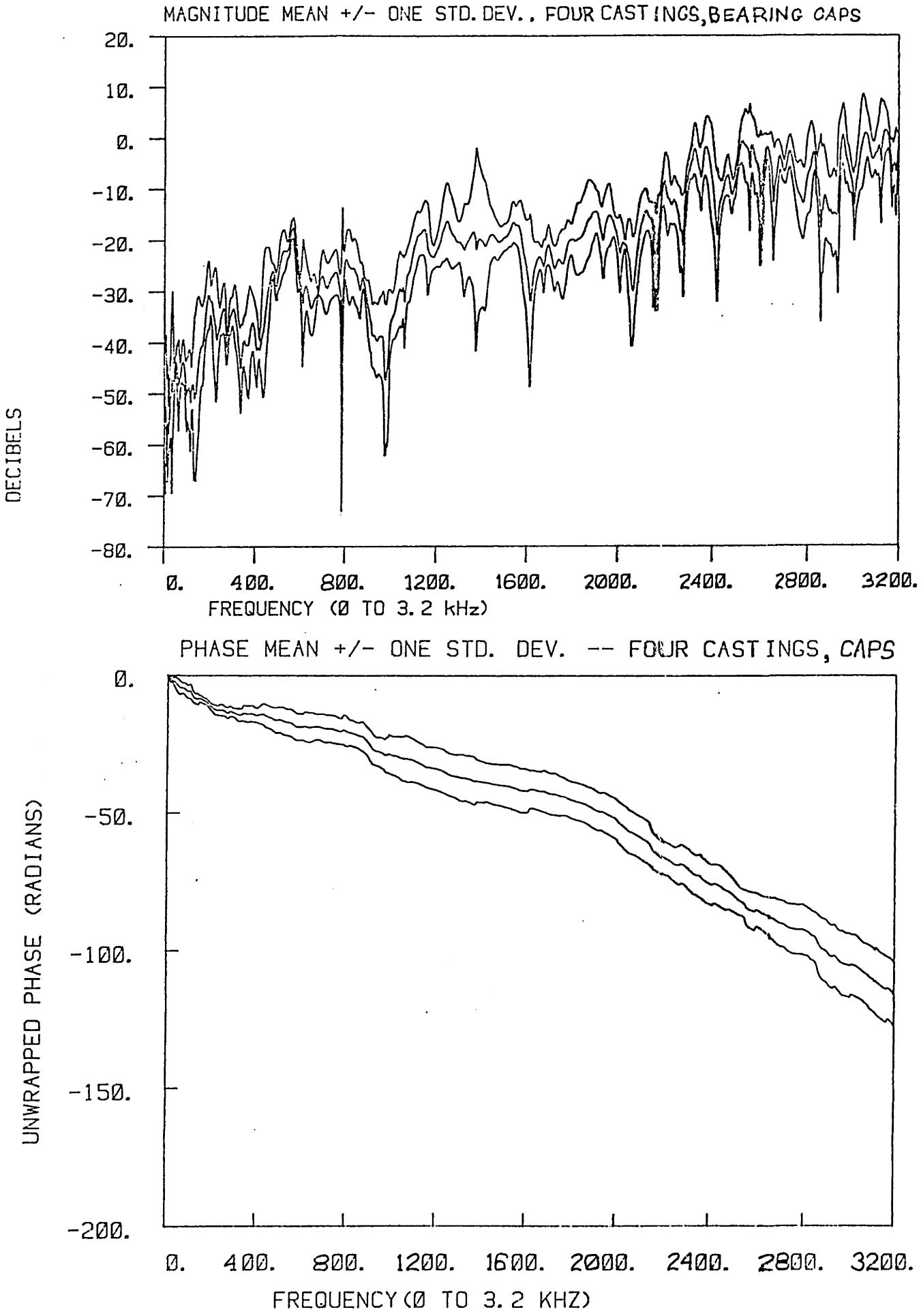

FIGURE 4.12 - Ensemble Statistics, Four Transfer Functions, Castings With Bearing Caps

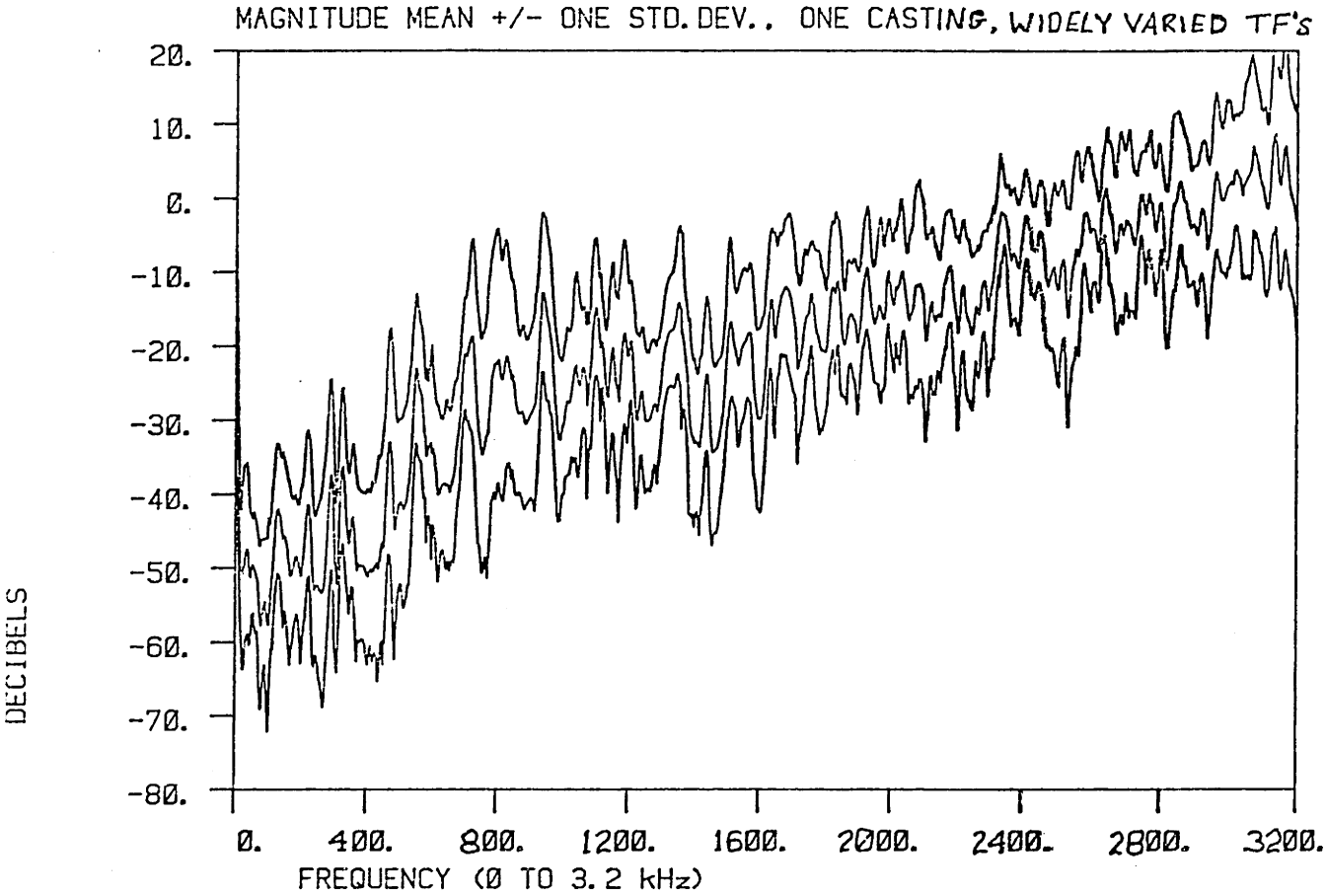

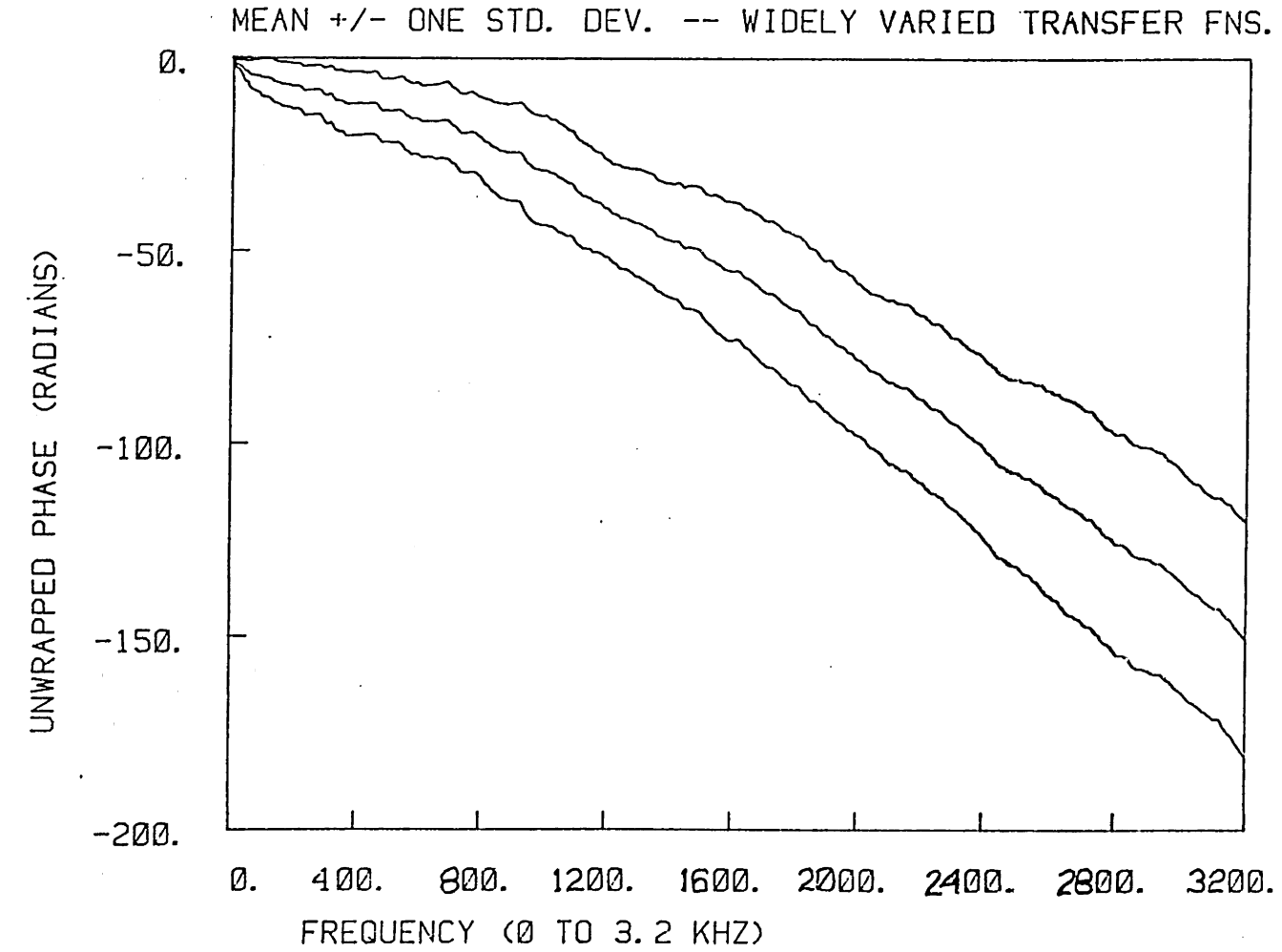

FIGURE 4.13 - Ensemble Statistics, One Casting,
Widely Varied Transfer Functions

CHAPTER 5

PROBABILISTIC ANALYSIS OF THE PHASE PROCESS

Since transfer functions seem to have considerable variation even under nearly ideal test conditions, it is worthwhile to attempt to develop some theory to predict the amount of variability. It is interesting that the standard deviation of magnitude is approximately constant with frequency, whereas the standard deviation of phase increases with frequency. It is important that any theory be consistent with these two observations.

5.1 VARIATIONS IN RESONANT FREQUENCIES

Even if the structures in a group are nominally identical, they are likely to have slight variations, perhaps due to material inconsistencies or other small differences resulting from the manufacturing process. Such differences could lead to small shifts in resonant frequencies and still leave the general frequency behavior unaffected. It has been stated before that modal density can be determined from large scale system parameters, but that precise prediction of

resonant frequencies is not generally feasible in a complex system. Structures with identical modal densities but with slightly different resonant frequencies will have slightly different transfer functions. Comparison of a mean magnitude curve, such as the castings curve in Figure 4.7, with an individual magnitude curve from the same ensemble, shown in Figure 1.1, indicates how resonant frequencies can vary. The peaks and dips are smoothed out, decreased in magnitude, in the mean calculation. This smoothing arises from variation in the frequencies of these resonances and antiresonances across an ensemble. The same variation in frequencies contributes to the high standard deviations in magnitude and phase of each ensemble.

Magnitude statistics of both the vibration of structures and the acoustical response of rooms have been greatly studied in the past. Random frequency spacing of resonances has been considered often, and the results indicate that amplitude variance should be constant over a wide frequency range. The theories are commonly called pulse arrival statistics. In the case of structures and rooms, the variance depends greatly on the modal overlap, a quantity proportional to the damping, which measures how much influence one resonant mode has on the response at nearby resonant frequencies [10].

5.2 RANDOM WALK MODEL FOR PHASE

A model for phase variability can be developed by considering the behavior of a single transfer function. If it is assumed that the modal density is the only characteristic known about the system, then the likelihood of a resonance occuring in a particular frequency interval can be determined through a probabilistic analysis.

The increasing standard deviation of the phase curves suggests that phase is governed by a probabilistic process. A process is usually an analysis of a system's behavior through time, where in a certain time interval, an event may or may not occur. A characteristic of a commonly studied process called a random walk is that any prediction of the state of a system can never be precise, but only statistical in nature, and that the precision of the prediction decreases with time. We can make a simple analogy and view the frequency axis of a transfer function as we are used to viewing a time axis. A step in frequency is comparable to a time step, so the occurence of a pole or a zero on the frequency axis is equivalent to an event occuring on a time scale. In Figure 5.1 is shown a series of steps on a frequency axis, some of which contain "events," occurences of poles and zeros.

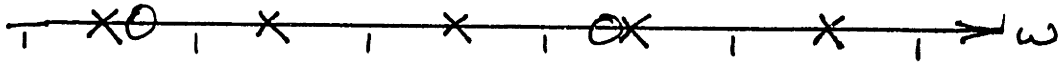

FIGURE 5.1 - Discrete Probabilistic Events on Frequency Axis

5.2.1 The Bernoulli Process

Since modal density is known for any given structure, it is convenient to simplify the model by assuming a regular occurence of poles. We can divide the frequency axis into units to make an analysis of a discrete process. In this case a frequency unit, equivalent to a time increment known as a trial in the probabilistic sense, is set equal to the average modal spacing. So in each frequency step of one unit a pole is assumed to occur with a probability of one, but a zero will not necessarily occur. Therefore it is simple to only consider the zeros in the process. It was shown in Chapter 2 that zeros are one-half as likely as poles, so the probability of a zero occupying any interval is 1/2. Figure 5.1 is an example of a series of discrete frequency intervals, every one of which contains a pole.

Considering the phase in the above model, in a frequency step where a pole alone occurs, there will be a phase change of -pi radians, whereas in a step where a zero also occurs, there will be no net phase change. This assumes that the zero and pole occur close together, or that, in other words, the phase step of every other pole is 'cancelled' by a zero.

Commonly in the analysis of processes, a successful trial is considered to have a value of 1, and an unsuccessful trial has a value of zero. The phase steps can be normalized by dividing by -pi, in which case a phase step of -pi due to an uncancelled pole has a value of 1. The probability model is

known as the Bernoulli random walk with probability p = 1/2. If we keep track of the sum of the trial results, then the result of the process is described probabilistically by the Binomial distribution. The most common example of this probability law in action is in the analysis of a series of coin tosses.

After n trials of a Bernoulli process, the mean value, or expected outcome, equals n x p. The variance, equal to the square of the standard deviation, is

$$\sigma^2 = n \times p \times (1-p) \qquad (5.1)$$

It is useful to compare the growth of the variance with the growth of the mean. The ratio

$$\sigma^2 / m = 1-p \qquad (5.2)$$

should be constant, equal to 1/2 for a Bernoulli probability of 1/2.

5.2.2 The Poisson Process

The Bernoulli model is somewhat restrictive in that it imposes discrete behavior on what in reality is a continuous process. By relaxing the restriction that poles appear at regular intervals, a model known as the Poisson process can be applied. A Poisson time process is characterized by a rate, λ, rather than a discrete probability. The rate describes the average number of successes (commonly called events or arrivals) per unit time. Therefore, the mean of a Poisson process equals $\lambda \times t$. Poisson's analysis is frequently applied to continuous series of randomly occurring events,

such as the arrival of telephone calls at a switchboard. In our case we consider random arrivals of 'cancelled' and 'uncancelled' poles, for which we know the average rates of occurence with frequency.

The variance of a Poisson process is equal to the mean, so

$$\sigma^2 / m = 1 \qquad (5.3)$$

This can be understood by considering the process to be equivalent to a binomial process with trials at infinitesimally small time intervals. As the interval size approaches zero, the Bernoulli probability of a success also approaches zero. Therefore, variance over mean, 1-p in the discrete case, approaches 1 in the Poisson process.

A further refinement of the analysis is made if the zeros and poles are assumed to be completely independent of each other. In this case, a zero is no longer assumed to cancel the phase step of a pole, but instead to cause a phase step of its own, one of +pi radians. The final phase value up to any frequency should be the same as in the previous model, but this model allows greater variability in the actual phase path.

In this normalized random walk model, two Poisson processes are occurring, the arrival of +1 (poles) and the arrival of -1 (zeros). The Poisson rate for zeros should equal one-half that of poles. The superposition of two Poisson processes has an arrival pattern which is also Poisson

in nature, and its rate is equal to the sum of the two component rates. If the net rate, λ, is the sum of $\lambda_p = p \times \lambda$ for poles and $\lambda_q = q \times \lambda$ for zeros, then p = 2/3 and q = 1/3 (since p + q = 1 and p = 2 x q). The characteristic function for this process has been derived [11] and is

$$\psi(\vartheta) = e^{\lambda t(pe^{i\vartheta} + qe^{-i\vartheta} - 1)} \qquad (5.4)$$

From the characteristic function can be calculated the moments of the distribution, where the nth moment is equal to the nth derivative of the characteristic, evaluated with the argument ϑ equal to zero. The first moment, or the mean, is

$$E[s] = \lambda \times t \times (p-q) \qquad (5.5)$$

and the second moment is

$$E[s^2] = \lambda \times t \times [1 + \lambda \times t \times (p-q)] \qquad (5.6)$$

The variance is defined as the difference between the second moment and the square of the first moment. In this case the variance equals λ x t. Therefore the variance divided by the mean equals 1/(p-q), or 3 for the process being considered.

5.3 ANALYSIS OF THE EXPERIMENTAL DATA

Values of variance divided by mean have been calculated for all the ensembles tested. These data are shown in Figures 5.2 through 5.6. The variance, σ^2, is defined as the mean-square deviation of data from the mean, described in Equation 4.1. Variance has been predicted to increase at the same rate as the mean, or linearly with frequency, so standard deviation should increase as the square root of frequency, which perhaps explains the observed standard deviation trend,

a rapid increase at low frequencies, followed by more gradual increase at higher frequencies. For phase data, the variance is in units of squared radians. To normalize the variance divided by mean data to fit the model of phase steps of pi radians, phase variance must be divided by pi times the mean, rather than just by the mean.

In each ensemble, the variance divided by mean curve is very roughly constant, as predicted, but there appears to be very little agreement with any particular process. For the large ensembles of castings and engines, shown in Figure 5.2, the curves lie near 1/2 and 1, respectively. This behavior could be compatible with the theory, as one might predict that similar castings or engines would have very similar resonant frequencies, or pole locations, but slightly different antiresonances, and that the behavior would approximate the binomial or simple Poisson model. The data from the small groups of castings with and without bearing caps, Figure 5.4, also support this conjecture. However, other data are less impressive. The pretest and posttest engines, shown in Figure 5.3, vary from around 1/2 to near 2, behavior which cannot be adequately explained by the same theory.

As expected, the curves for a single casting with only slight shaker or accelerometer movements are quite low, in Figure 5.5, reflecting measurement error. The group of 25 widely varied transfer functions on a single casting, Figure 5.6, shows data relatively constant between 1.5 and 2. In these measurements, the locations of resonances should be

similar, since the same structure was always under test, but the antiresonances, or zeros, should be widely scattered. This seems to be an ideal case for the Poisson model, but the values are a bit high. However, it is encouraging that none of the values in this or any other curve exceeds 3, the theoretical upper bound established by the dual process random walk model.

It appears that the probability models, developed in accordance with the theory of transfer function phase in Chapter 2, have little predictive value toward statistics of actual data. Some arguments for why the theory might not be entirely accurate are presented in the following chapter.

5.2)

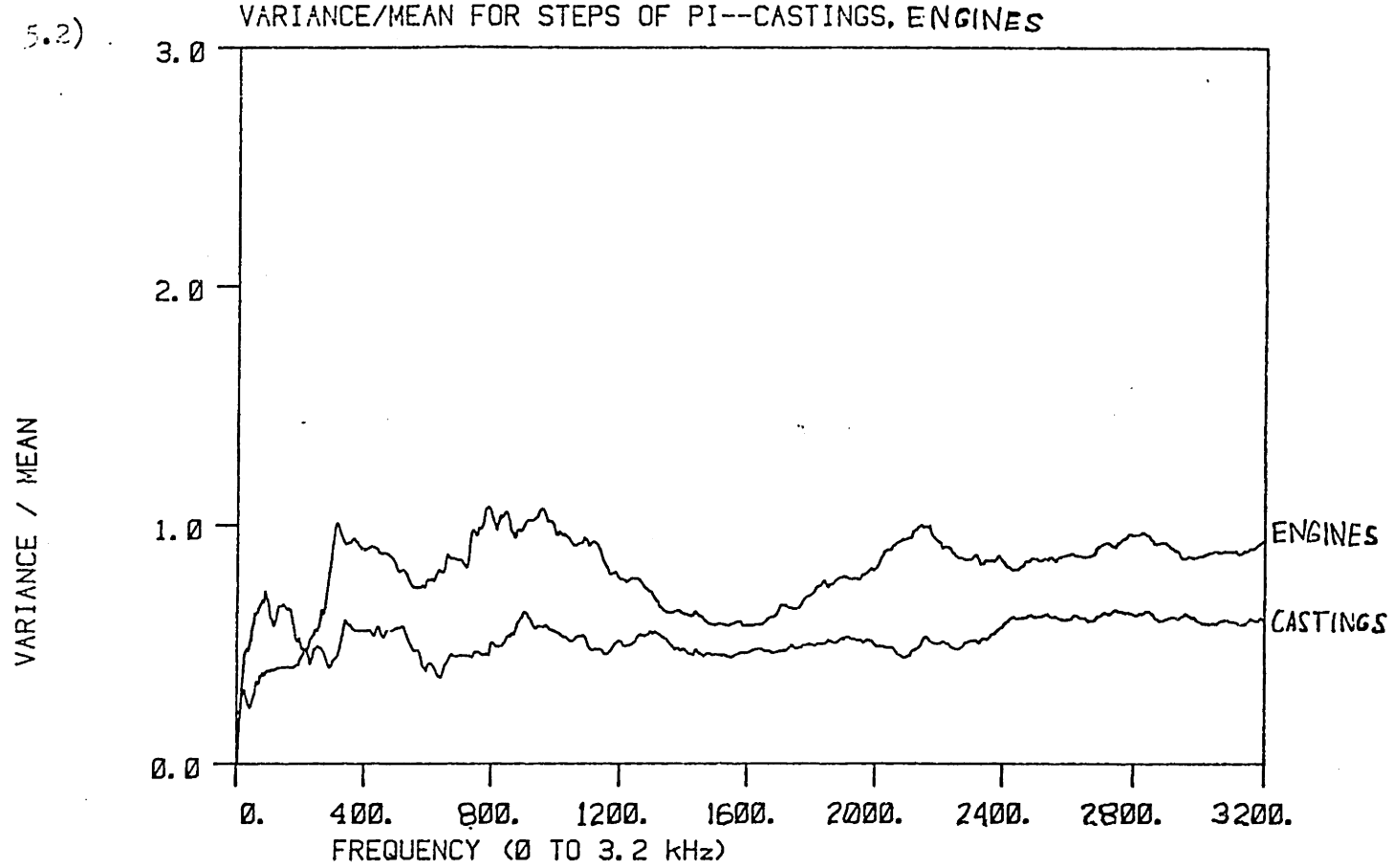

5.3)

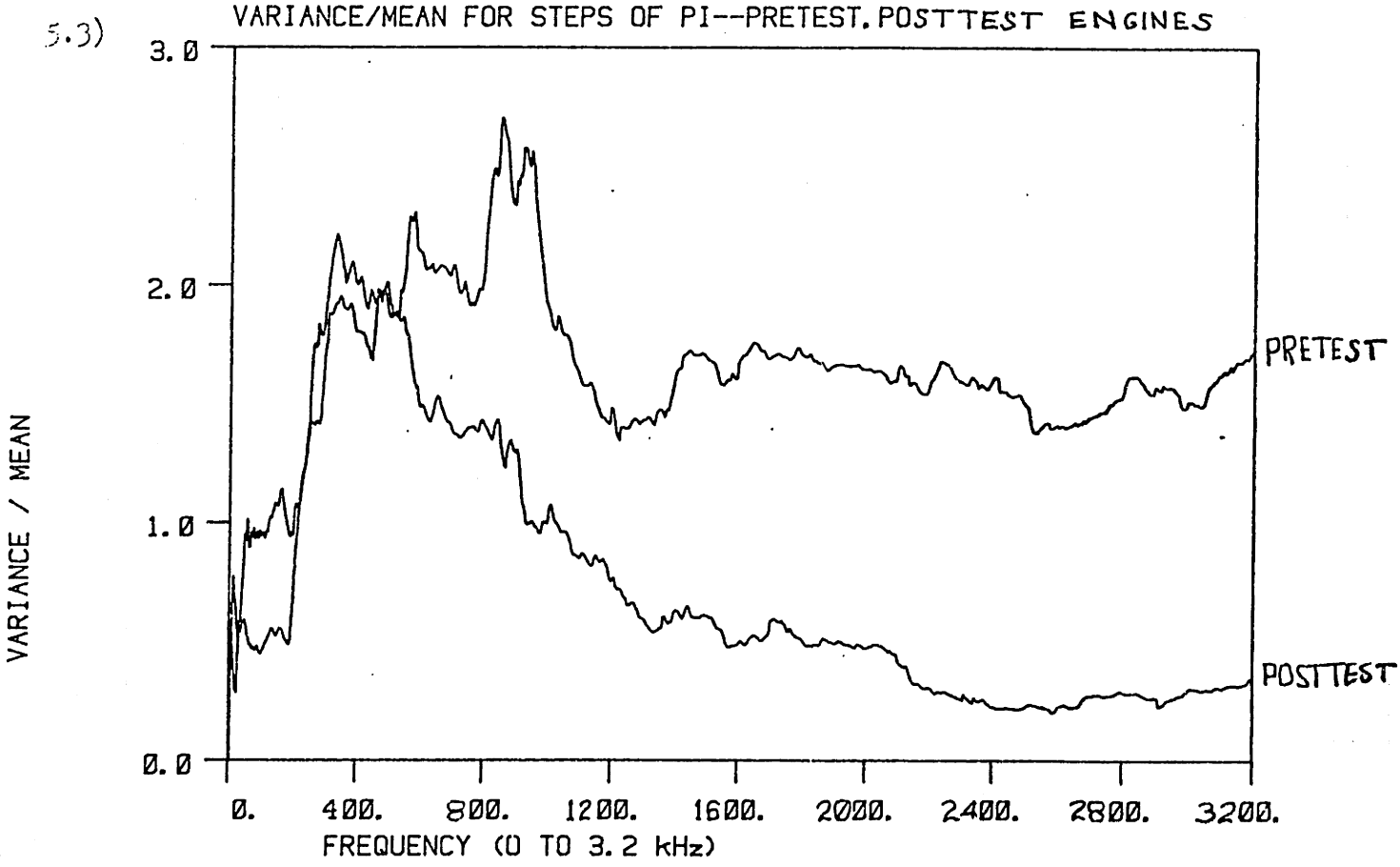

FIGURES 5.2 and 5.3 - Variance Divided by Mean of Unwrapped Phase,
-Castings and Engines
-Pretest and Posttest Engines

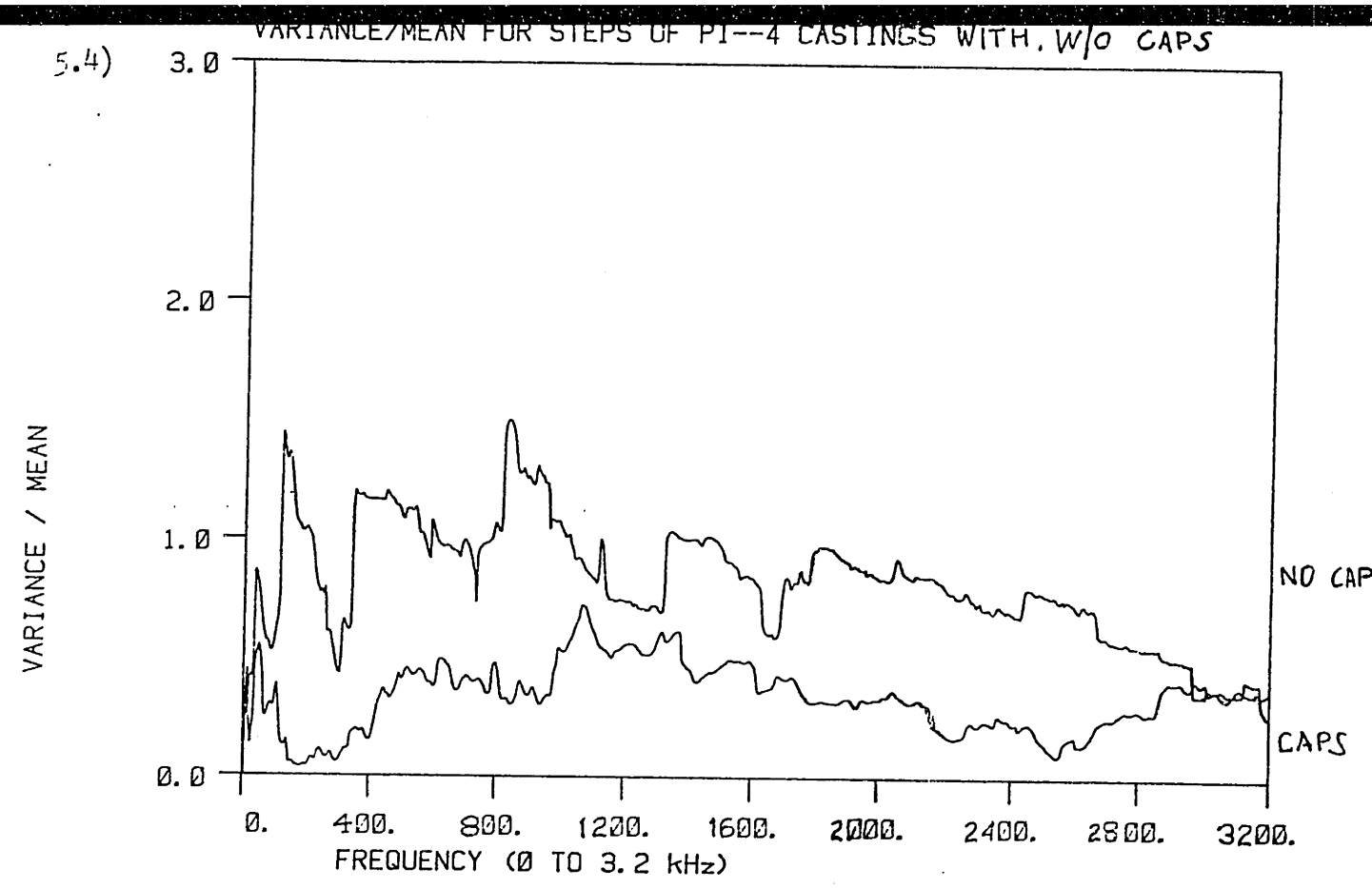

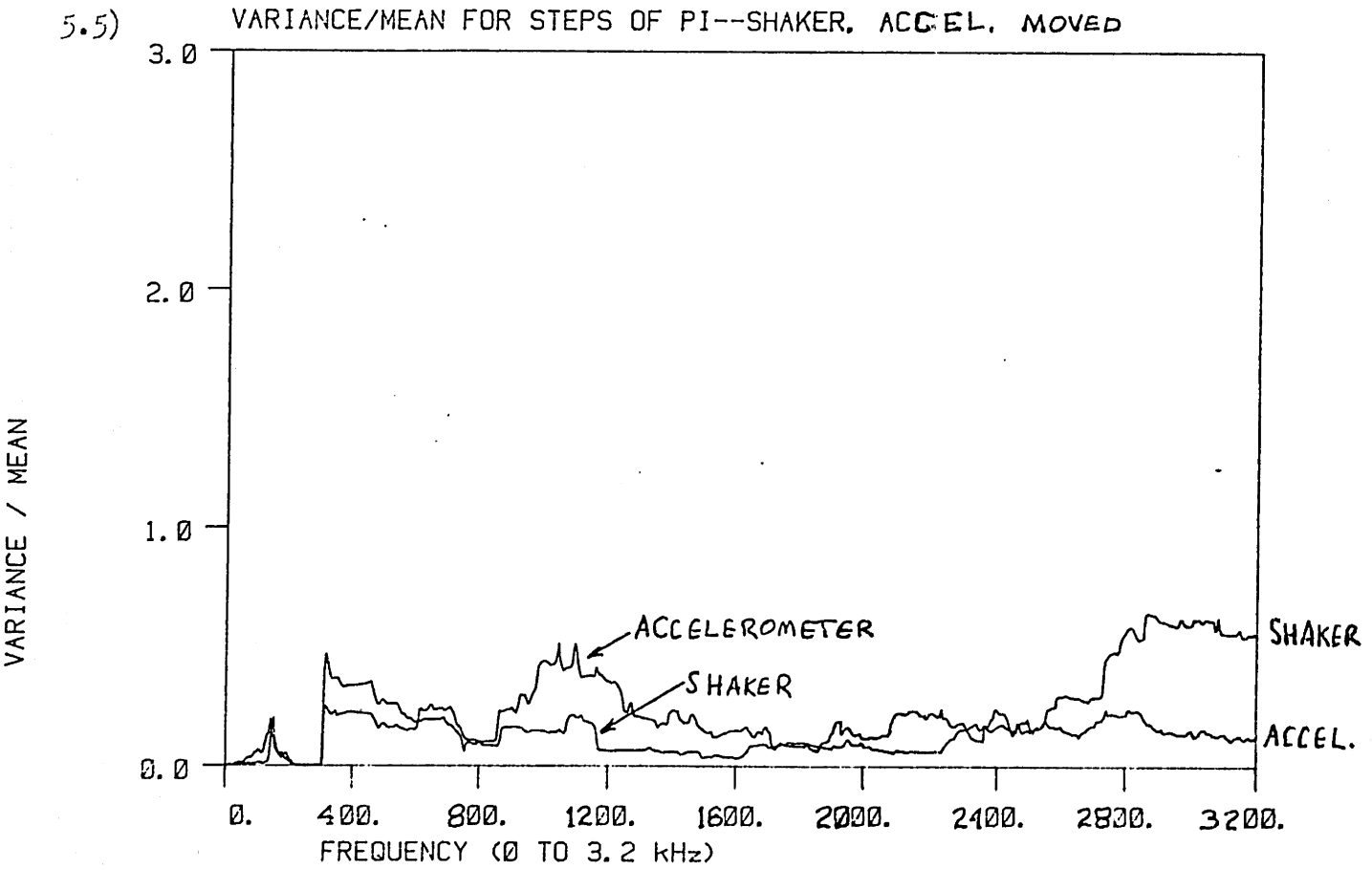

FIGURES 5.4 and 5.5 - Variance Divided by Mean of Unwrapped Phase,
-Four Transfer Functions, Castings With and Without Bearing Caps
-One Casting; Shaker Moved Slightly and Accelerometer Moved Slightly

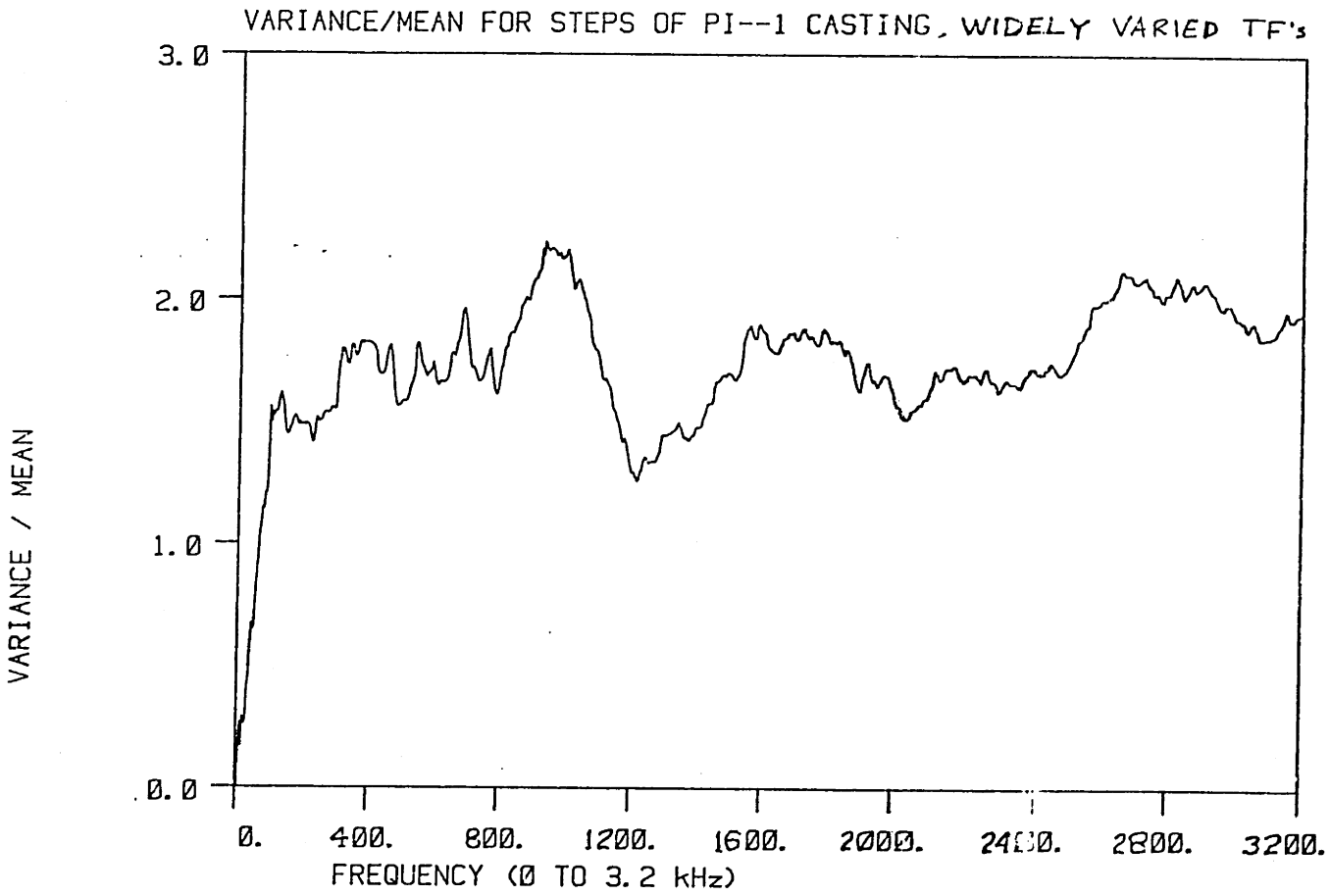

FIGURE 5.6 - Variance Divided by Mean of Unwrapped Phase, One Casting, Widely Varied Transfer Functions

CHAPTER 6

THE MINIMUM PHASE CONDITION

The discrepancies in both mean and variance of unwrapped phase among the ensembles of engines described here suggest that there may be contributions to phase spectra other than those described in Chapter 2. Particular attention is paid in this chapter to the possibilities of "double zeros" and "non-minimum-phase zeros" in transfer functions.

6.1 DOUBLE ZEROS

In the discussion of the occurence of zeros, in Chapter 2, it was assumed that, at any frequency, the "remainder" term in the modal expansion is negligibly small compared to the terms from the two nearest resonant modes. The remainder term represents the net contributions of modes resonating at all other frequencies, and is large in the case of high modal overlap. In some cases both the remainder and the two dominant terms must be considered.

In Figure 6.1 is shown a frequency region where the two dominant modal terms would not ordinarily add to zero. However, the addition of a positive remainder term causes the sum to equal zero at two points very close to each other on the frequency axis [8]. This condition is known as a double zero. Its effect on a transfer function is to cause a very deep minimum in the magnitude and a contribution of +(2 x pi) to the phase, one +pi for each zero. Although a double zero was not directly accounted for in the phase processes derived in Chapter 5, it can easily result in the Poisson model with independent arrivals of poles and zeros, simply by having one zero arrive immediately after another.

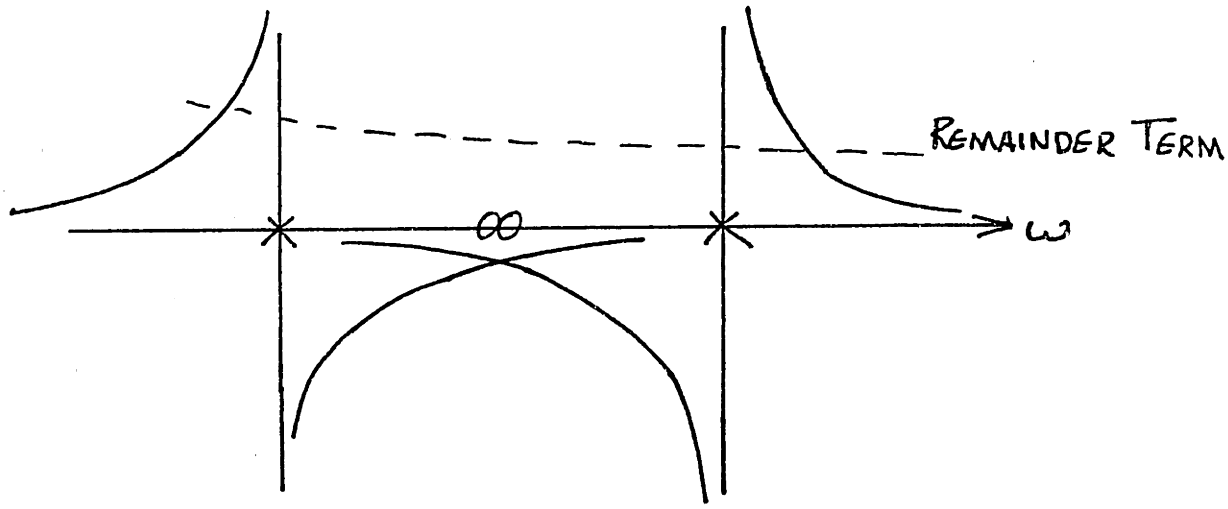

FIGURE 6.1 - The Occurence of a Double Zero

6.2 NON-MINIMUM-PHASE ZEROS

Up to this point, it has been assumed that zeros, like poles, must have positive imaginary parts, and thus lie above the real frequency axis. A system with only these zeros is

called minimum-phase, since, for the given magnitude, the net phase delay is minimum. If some of these zeros were below the real axis, then the magnitude would be the same, but the phase delay would increase by 2 x pi for each such zero; that is, the unwrapped phase would change by -(2 x pi) for each of these zeros. Zeros obeying this property are called non-minimum phase. A non-minimum-phase zero is shown, with the phasor angle which determines the phase contribution, in Figure 6.2 [8].

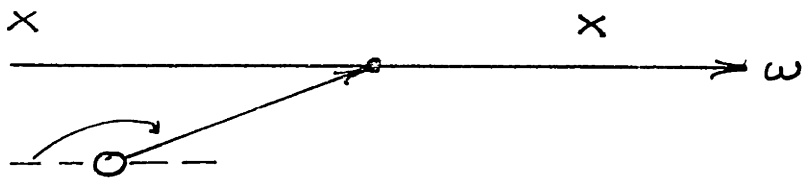

FIGURE 6.2 - Non-Minimum-Phase Zero in Frequency Plane

For a minimum-phase system, the system inverse, like the system itself, is both causal and stable. This is because the zeros of a system become the poles of a system inverse, and vice versa. Non-minimum-phase zeros would become unstable poles in a system inverse [4].

An important property of a system which obeys the minimum-phase condition is that the magnitude and phase of the system are related by the Hilbert Transform. If the Hilbert Transform, defined such that

$$H_{im}(e^{j\omega}) = \begin{cases} -j\,H_{re}(e^{j\omega}) & , \; 0 \le \omega < \pi \\ j\,H_{re}(e^{j\omega}) & , \; -\pi \le \omega < 0 \end{cases} \qquad (6.1)$$

is applied to the log magnitude of a minimum-phase transfer

function, then the unwrapped phase is the result [4]. For such a system, only the magnitude would have to be measured experimentally, which is a valuable consequence. However, it has never been proven that the minimum-phase condition applies to physical systems such as structural transfer functions.

6.3 EXAMINATION OF ZEROS IN TRANSFER FUNCTION DATA

Much of the data studied here was examined closely in an attempt to identify anomalies in phase spectra around transfer function zeros. It was suspected that ensembles such as the pretest engines, which displayed low values of unwrapped phase but relatively high variance, might contain transfer functions with double zeros. However, although deep notches often occur in magnitude spectra, a jump of +(2 x pi) was never found in any phase curve.

In some of the data from the castings without bearing caps, the structures which should have the lowest damping, and those which should obey the two-dimensional theory the best, some evidence suggesting non-minimum-phase zeros was found. Recall from Figure 4.12 that the group of four transfer functions on castings without caps had the greatest mean unwrapped phase, which could suggest the greatest frequency of non-minimum-phase zeros. In Figure 6.3 is shown a detail from a transfer function on a casting without caps, one of the 25 transfer functions with widely varied measurement points. The pole-zero-pole combination at about 300 Hz clearly causes a phase advance of approximately -(3 x pi) radians, strongly

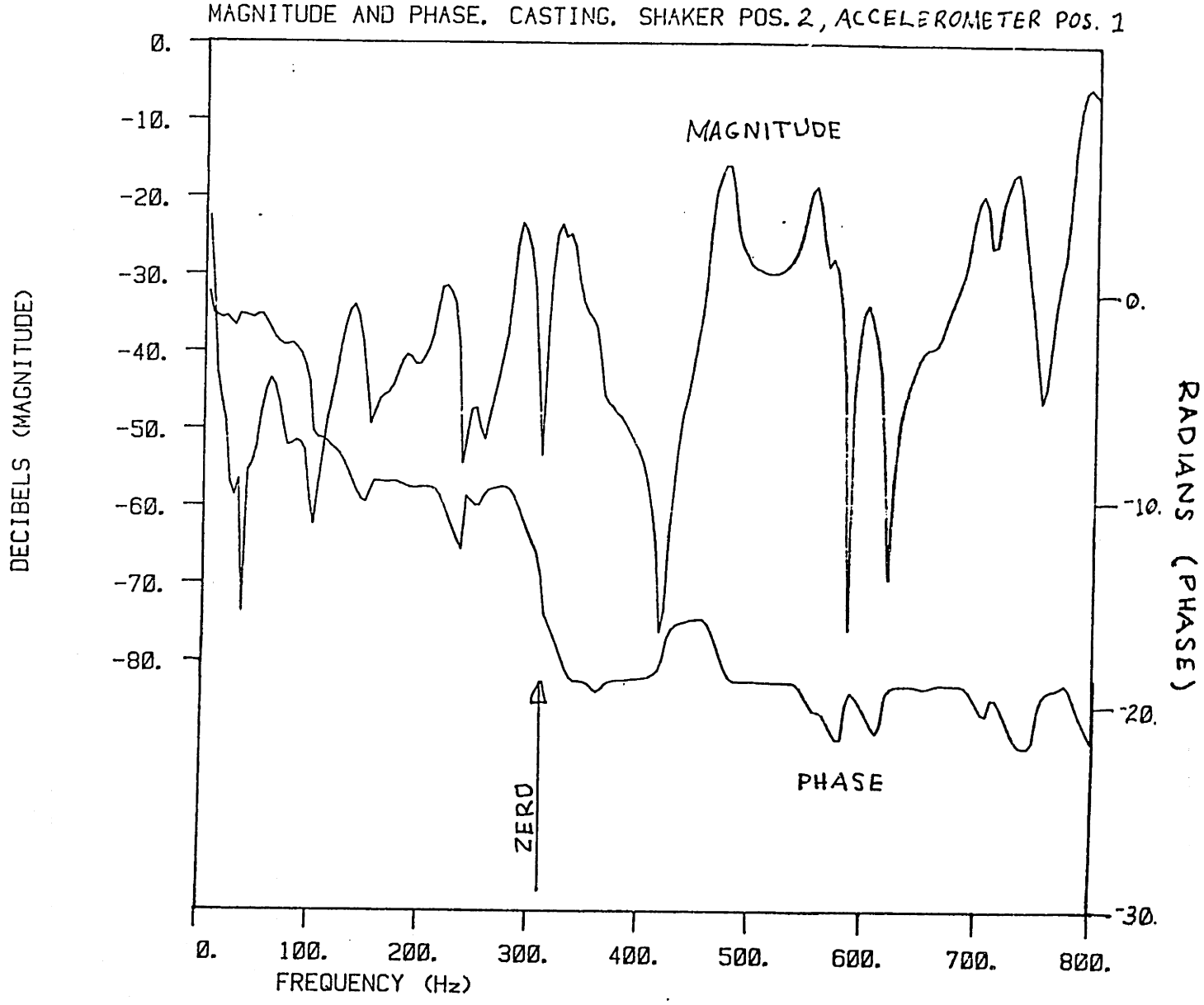

FIGURE 6.3 - Transfer Function Detail, Casting Without Bearing Caps

suggesting that the zero is not minimum-phase. The phase behavior around the zero at 100 Hz is also unusual, although less convincing.

One of the castings from the group of four without bearing caps for which measurement locations were not changed showed unusual phase behavior at low frequencies, as shown in Figure 6.4. The phase for this casting, identified as #1, advances by approximately 20 radians more than any of the other three between 0 and 400 Hz. An examination of the magnitude curves of castings 1 and 2, in Figure 6.5, show the existence of about 7 zeros in casting 1 that are not present in casting 2. The possibility of 7 non-minimum-phase zeros, which would result in -(7 x pi) radians of phase, is consistent with the measured discrepancy of about 20 radians. Again, the zero at 300 Hz in casting 1 is especially convincing evidence for non-minimum-phase behavior, as can be seen in Figure 6.6.

Since a physical mechanism for the occurence of non-minimum-phase zeros has never been explained, it was suspected that some experimental anomaly, perhaps loose shaker contact, could cause the appearance of so many unusual zeros in the transfer function of casting #1 described above. In an attempt to identify an inconsistency, the data were used to determine the system impulse response, related to the transfer function itself by the inverse Fourier Transform. Particularly useful was the impulse response envelope, or energy-time curve, determined by use of the Hilbert Transform.

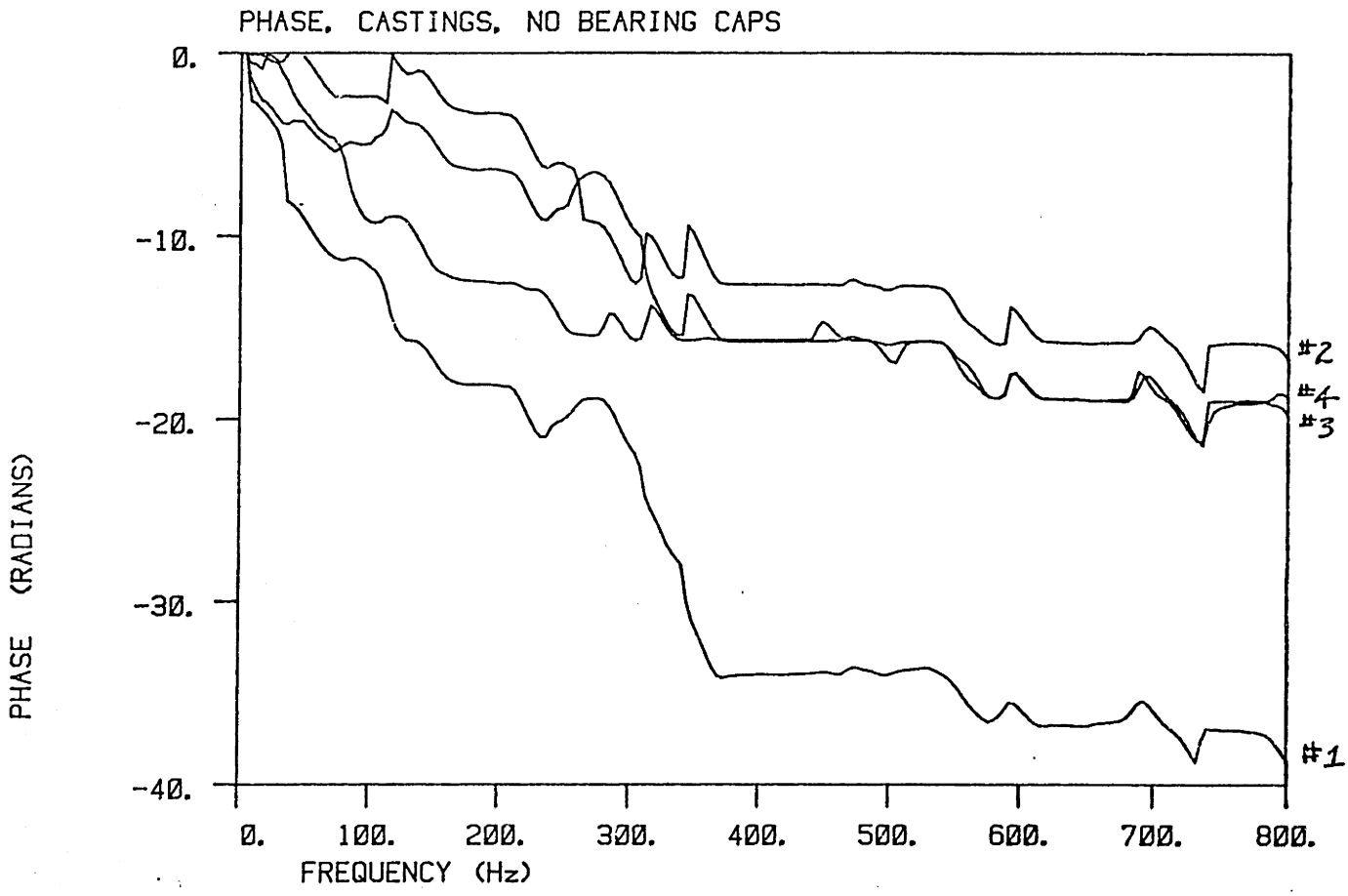

FIGURE 6.4 - Phase Detail, Four Transfer Functions, Castings Without Bearing Caps

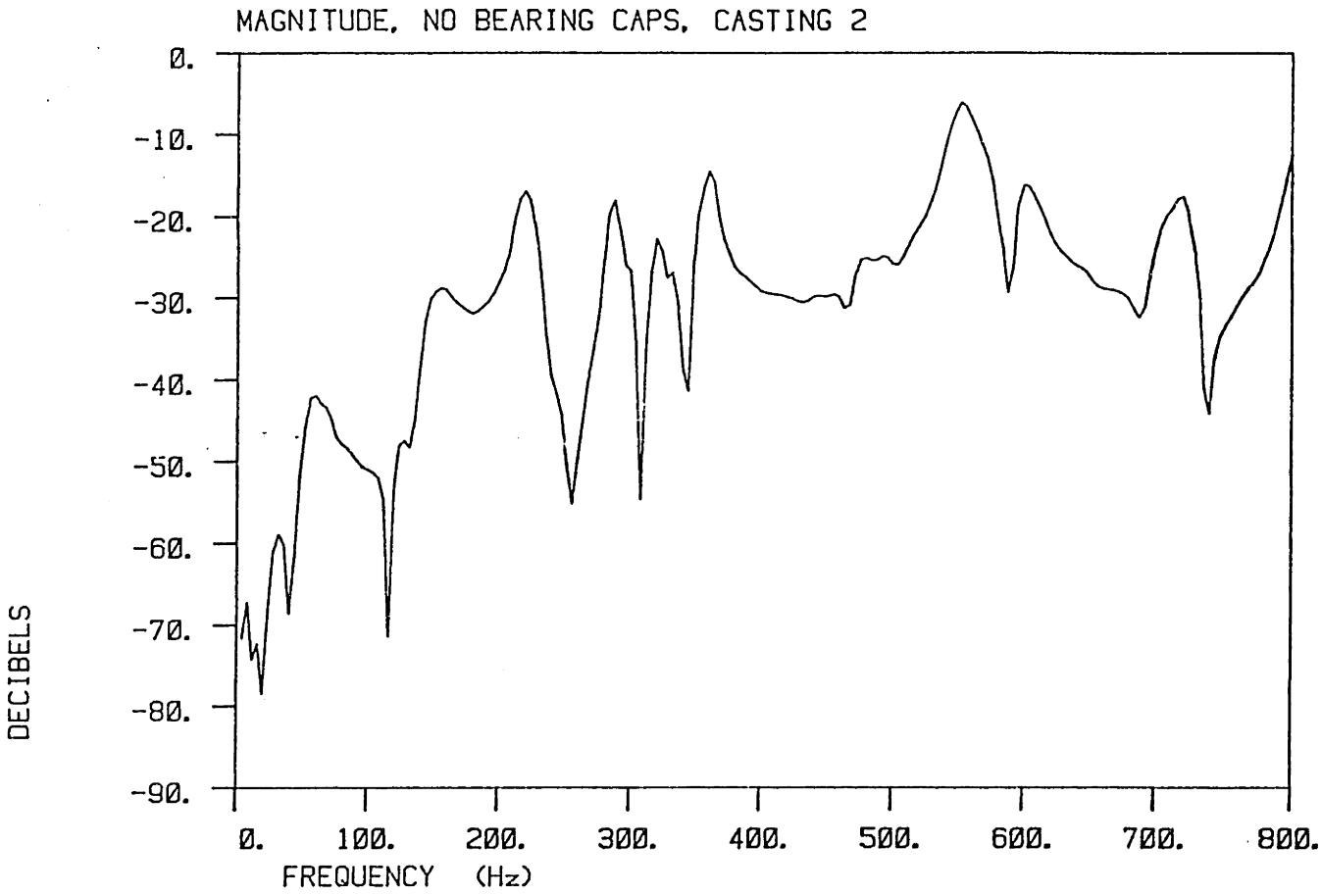

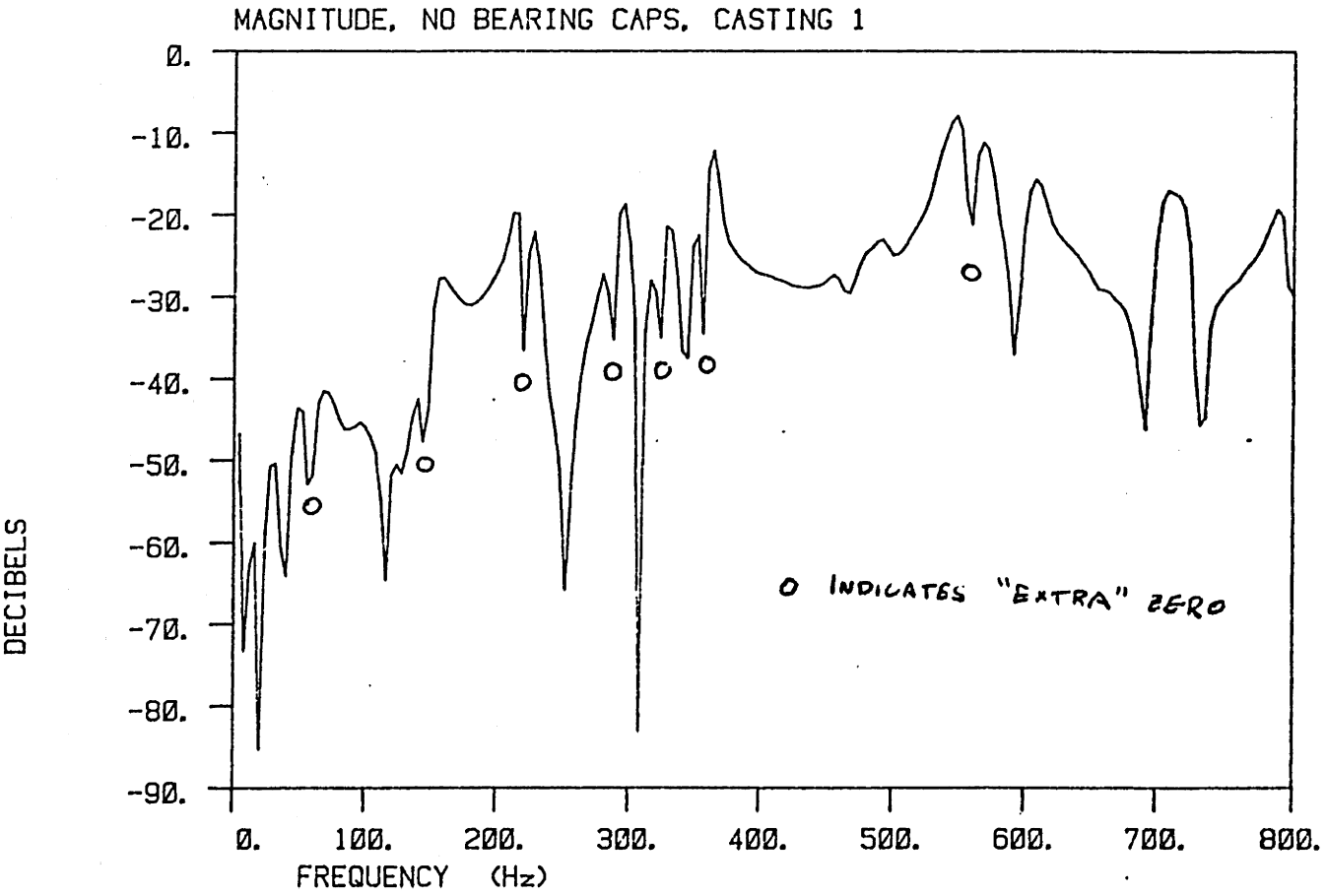

FIGURE 6.5 - Magnitude Detail, Two Transfer Functions, Castings Without Bearing Caps

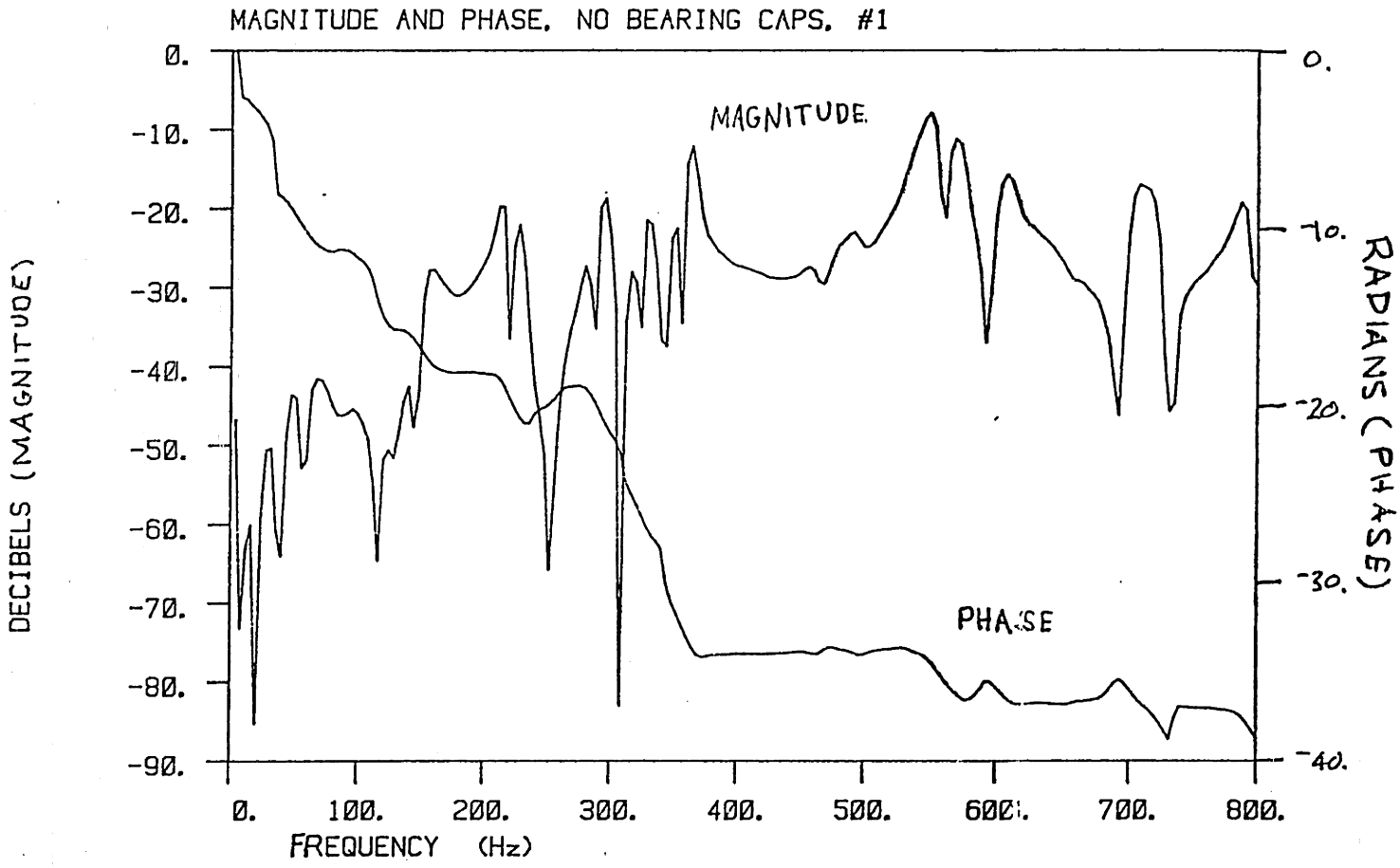

FIGURE 6.6 - Transfer Function Detail, Casting Without Bearing Caps

This analysis provided no clue as to the reason for the presence of the zeros, as all of the envelopes looked quite similar. Inaccurate phase unwrapping was also suspected; however, the transfer functions which exhibited non-minimum-phase behavior were among those studied when the unwrapping program was tested successfully for consistency.

The possibility that non-minimum-phase zeros may exist in the simple casting structures may help to explain why the mean unwrapped phase for the ensemble of castings is so much greater than for any of the assembled structures. It can be seen from the mean phase curves in Figures 4.7 through 4.10 that, up to about 1500 Hz, the phase trend is similar for all the ensembles; however, above this frequency the phase for castings diverges. Comparison of the mean magnitude curves in these same figures reveals some strong zeros in the high frequency portion of the mean of the castings' spectra. It is possible that these zeros could be non-minimum-phase.

The Hilbert Transform was applied to some of the transfer functions to learn how well magnitude could be reconstructed from phase, and vice versa, a test of the minimum-phase condition. The unwrapped phase of a minimum-phase transfer function is the sum of a linear term and a term representing fluctuations about the linear phase. A linear phase spectrum corresponds to a pure time delay of a signal [4]; therefore it cannot be identified from a magnitude spectrum. If the minimum-phase condition is satisfied, the Hilbert Transform of the magnitude should equal the fluctuation component of the

phase, and vice versa. It was found that when this operation was applied to individual transfer functions the results did not agree, again suggesting that the mimimum-phase condition may be violated.

CHAPTER 7

CONCLUSIONS AND RECOMMENDATIONS

It is encouraging that the unwrapped phase curves from the 1985 data seem to agree approximately with the values estimated from predicted modal density, for this suggests that the experimental procedure is resulting in data of good quality. But the conclusion to be drawn from the high levels of phase variability must be the same as that from the 1983 data, that a single transfer function cannot be generalized to a robust inverse filter for an ensemble of structures, even under controlled conditions. Therefore it is essential that future diagnostics research should concentrate on the development of techniques for adaptive inverse filtering, in which the transfer function used for filtering is adapted to each individual machine.

More work is needed to learn why the levels of unwrapped phase change as the complexity of the machine changes. It is puzzling that the ensemble of castings shows so much more phase delay than the ensembles of engines, which of course were constructed from similar castings. The wave propagation

properties of assembled machines may not obey two-dimensional plate theory as closely as the castings. Perhaps other propagation paths exist in the assembled engines to account for the difference in phase behavior.

The random walk model for frequency dependence of phase provides accurate information about the approximate level of phase variability, but it is not precise enough to be used to predict variability. Continued study of the fundamental phase behavior of transfer functions will help to explain variability. The experimental data can be used to provide further insight into the validity of the probabilistic model, such as a study of whether the phase process shows stationary and ergodic behavior with respect to frequency.

Additional data from simple structures such as flat plates will help in the refinement of the phase theory. Additional experiments should also improve our understanding of the behavior of transfer function zeros. An experiment to produce a transfer function with double zeros should be conducted in order to test the unwrapping algorithm. It is possible that the algorithm is not capable of recognizing double zeros in transfer functions.

Finally, future transfer function data should be examined closely to learn more about the possibility of non-minimum-phase zeros. The Hilbert Transform relation between magnitude and phase should be tested much more on the 1985 data, and on any future data, since it is a good way to study minimum phase properties.

APPENDIX

A CATALOG OF THE 1985 DATA SET

CASTINGS

45 Transfer functions.

Engine castings with bearing caps mounted.

Identified as CAST1, ... , CAST52.

Files lost due to tape failure: 15, 24, 30, 44.

Files not included in ensemble due to unsuccessful phase unwrapping (unwrapping was later solved.): 23, 38, 45.

ENGINES

43 Transfer functions.

Partially assembled engines on assembly line.

Identified as ENG1, ..., ENG60.

Files lost: 6, 21, 22, 27, 29, 30, 31, 32, 33, 34, 39, 41, 42, 45, 46, 47.

File not included: 23.

PRETEST

12 Transfer functions.

Completed engines, just off assembly line, mounted on test stands.

Identified as PRE1, ..., PRE12.

POSTTEST

12 Transfer functions.

Completed engines, just after first test operation, mounted on test stands.

Identified as POST1,..., POST12.

WITH BEARING CAPS

4 Transfer functions.

4 Castings with bearing caps mounted.

Not included in CASTINGS Ensemble.

Identified as BC1 (Engine serial #3321), BC2 (#3408), BC3 (#4180), BC4 (#754).

Note: These castings were the first ones measured. Shaker and Accelerometer positions were not carefully recorded; the positions may well have been different from CASTINGS ensemble and NO BEARING CAPS ensemble.

NO BEARING CAPS

4 Transfer functions.

2 Castings with bearing caps and bolts removed.

Identified as NBC1 (#754), NBC2 (#3321), NBC3 (#3321), NBC4 (#754).

SHAKER MOVED

5 Transfer functions.

Casting #3321 with bearing caps removed.

Accelerometer held fixed, shaker moved slightly each time (approximately 1 cm.)

Identified as SMOV1, ..., SMOV5.

ACCELEROMETER MOVED

4 Transfer functions.

Casting #3321 with bearing caps removed.

Shaker held fixed, accelerometer moved slightly.

Identified as AMOV1, ..., AMOV5.

File lost: 2.

WIDELY VARIED

24 Transfer functions.

Casting #3321 with bearing caps removed.

Five shaker positions, five accelerometer positions arbitrarily chosen. 25 Transfer functions measured, all different.

Identified as A1S1, ..., A5S5.

File lost: A3S1.

REFERENCES

Ordubadi, A., "Component and Fault Identification in a Machine Structure Using an Acoustic Signal," ScD Thesis, Department of Mechanical Engineering, MIT, May 1980.

Bowen, D., "Application of Signature Inverse Filtering to the Fault Diagnosis of an Impact Mechanism," MSc Thesis, Department of Mechanical Engineering, MIT, March 1983.

Murville, M.L.A., "The Design of a Robust Inverse Filter for High Level Diagnostics," MSc Thesis, Department of Mechanical Engineering, MIT, March 1984.

Oppenheim, A.V. and Schafer, R.W., Digital Signal Processing, Prentice-Hall, Inc., Englewood Cliffs, NJ, 1975.

Lyon, R.H. and Ordubadi, A., "Use of Cepstra in Acoustical Signal Analysis," Journal of Mechanical Design, Vol.104, pp.303-306, April 1982.

Tribolet, J.M., "A New Phase Unwrapping Algorithm," IEEE Transactions on Acoustics, Speech, and Signal Processing, Vol.ASSP-25, No.2, pp.170-177, April 1982.

Smith, P.W.Jr., and Lyon, R.H., Sound and Structural Vibration, NASA Contractor Report #CR-160, March 1965.

Lyon, R.H., "Progressive Phase Trends in Multi-Degree-of-Freedom Systems," Journal of the Acoustical Society of America, Vol.73, No.4, pp.1223-1228, April 1983.

Lyon, R.H., "Range and Frequency Dependence of Transfer Function Phase," Journal of the Acoustical Society of America, Vol.76, No.5, pp.1433-1437, November 1984.

Lyon, R.H., "Statistical Analysis of Power Injection and Response in Structures and Rooms," Journal of the Acoustical Society of America, Vol.45, No.3, pp.545-565, March 1969.

Larson, H.J. and Shubert, B.O., Probabilistic Models in Engineering Sciences , Vol.2, John Wiley and Sons, New York, 1979.